*JBMR Plus*, 2025, **9**, ziaf048
https://doi.org/10.1093/jbmrpl/ziaf048
Advance access publication: March 29, 2025
**Research Article**

# Porcupine inhibition enhances hypertrophic cartilage differentiation

**Michael Killinger[1,†], Tereza Szotkowská[1,†], Denisa Lusková[1], Nikodém Zezula[2], Vítězslav Bryja[2], Marcela Buchtová[1,2,*]**

[1]Laboratory of Molecular Morphogenesis, Institute of Animal Physiology and Genetics, Czech Academy of Sciences, 602 00 Brno, Czech Republic
[2]Department of Experimental Biology, Faculty of Sciences, Masaryk University, 62504 Brno, Czech Republic

*Corresponding author: Marcela Buchtová, Laboratory of Molecular Morphogenesis, Institute of Animal Physiology and Genetics, v.v.i. Czech Academy of Sciences, Veveri 97, 602 00 Brno, Czech Republic (buchtova@iach.cz).

†Shared first authorship.

## Abstract

Porcupine (PORCN) is a membrane-bound protein of the endoplasmic reticulum, which modifies Wnt proteins by adding palmitoleic acid. This modification is essential for Wnt ligand secretion. Patients with mutated PORCN display various skeletal abnormalities likely stemming from disrupted Wnt signaling pathways during the chondrocyte differentiation. To uncover the mechanism of PORCN action during chondrogenesis, we used 2 different PORCN inhibitors, C59 and LGK974, in several model systems, including micromasses, 3D cell cultures, long bone tissue cultures, and zebrafish animal model. PORCN inhibitors enhanced cartilaginous extracellular matrix (ECM) production and accelerated chondrocyte differentiation, which resulted in the earlier induction of cellular hypertrophy as well as cartilaginous mass expansion in micromass cultures and cartilaginous organoids. In addition, both PORCN inhibitors expanded the hypertrophic zone and reduced the proliferative zone in the growth plate. This led to a significant increase in cartilaginous tissue and ultimately resulted in the elongation of tibias in the mouse organ cultures. Also, LGK974 treatment of *Danio rerio* embryos induced expansion of craniofacial cartilage width together with the shortening of the body axis, which was consistent with a phenomenon occurring upon inhibition of non-canonical Wnt signaling. By combining PORCN inhibition with exogenous Wnt proteins activating either canonical/$\beta$-catenin (WNT3a) or non-canonical (WNT5a) signaling, we propose that the key mechanism mediating pro-chondrogenic effects of PORCN inhibition is the removal of canonical ligands that prevent chondrocyte differentiation. In summary, our results provide evidence of the distinct role of PORCN in both the early and late stages of cartilage development. Further, our data demonstrate that PORCN inhibitors can be used in the experimental and clinical strategies that need to trigger chondrocyte differentiation and/or cartilage outgrowth.

**Keywords:** porcupine, Wnt, chondrogenesis, cartilage, hypertrophy, tibia, micromass cultures, orofacial anomalies, jaw hypoplasia

## Lay Summary

PORCN enables the attachment of palmitoleic acid to Wnt proteins, a crucial modification required for the secretion of all Wnt proteins. We uncovered that PORCN plays a crucial role in several differentiation events during cartilage development through its essential contribution to Wnt signaling. This is underlined also by the high incidence of skeletal abnormalities in FDH patients with mutations in PORCN. Our study revealed that PORCN inhibitors stimulate chondrocyte differentiation and hypertrophy by releasing the inhibitory effect of Wnt signaling. The pro-chondrogenic effect of PORCN inhibition was found across different stages of chondrogenesis, starting with increased expression of early genes essential for chondrocyte differentiation to enhancement of cartilaginous mass production in micromasses, tibiae, and organoids. As aberrant regulation of chondrocyte hypertrophy contributes to skeletal disorders, understanding factors that regulate this process can lead to the development of new therapies. In this light, PORCN inhibitors can be effectively used to fine-tune chondrocyte differentiation, which will benefit the field directing to enhance cartilage regeneration.

**Received:** September 7, 2024. **Revised:** March 15, 2025. **Accepted:** March 23, 2025

## Graphical Abstract

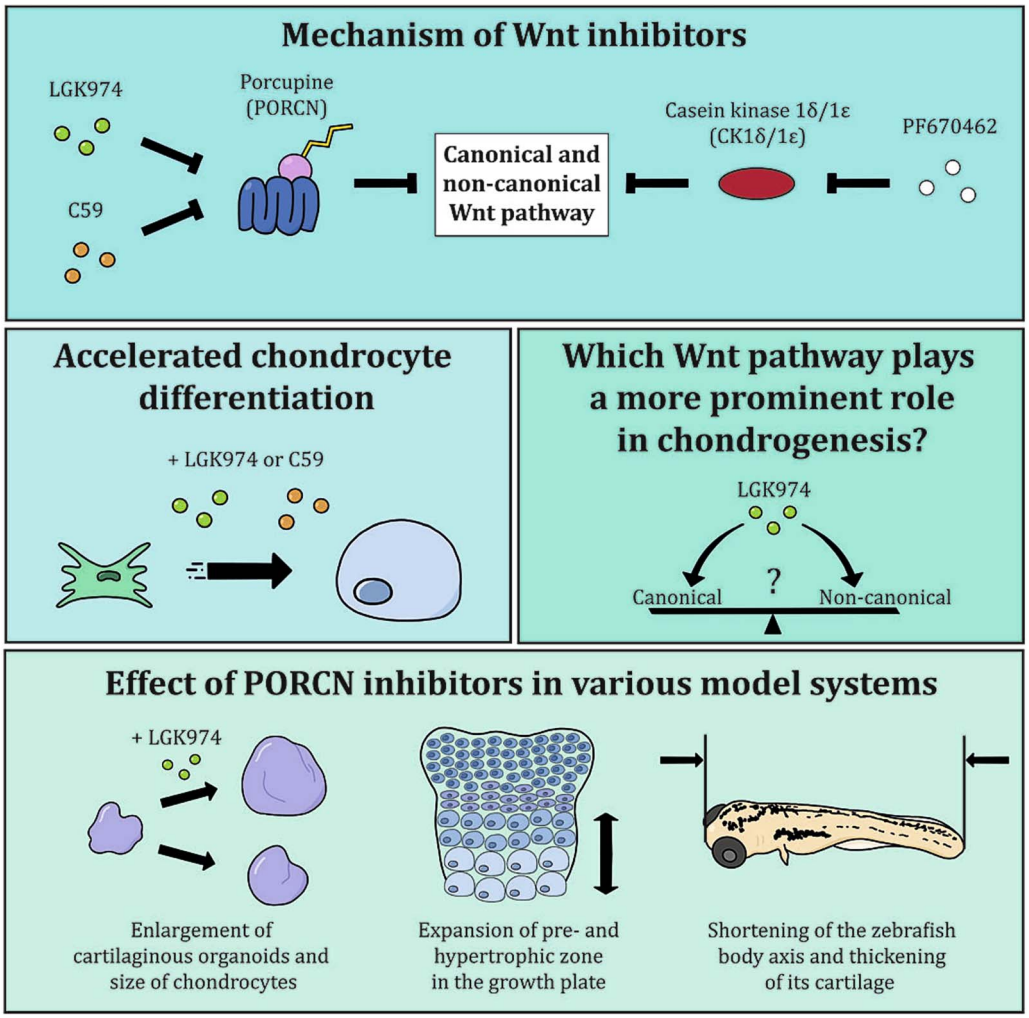


## Introduction

Cartilage development is a highly regulated process that involves coordinated action of systemic and local signals. Among these factors, Wnt family members play a critical role[1] and serve as effective agents for the regeneration of adult cartilaginous tissue.[2] Ectopic activation of the canonical $\beta$-catenin signaling pathway through WNT3a inhibits differentiation of mesenchymal progenitors by stabilizing intercellular contacts[3] and synergizes with BMP2 to promote ossification.[4] In contrast, inhibition of $\beta$-catenin leads to ectopic cartilaginous nodules,[5] indicating the essential role of $\beta$-catenin in early chondrocyte differentiation. Moreover, the non-canonical signaling pathway promotes cartilage formation, and WNT5a, the primary ligand controlling the non-canonical/planar cell polarity (PCP) Wnt pathway, regulates the chondrocyte's transition from the resting to the proliferative zone and maturation into hypertrophic cells. WNT5a is presumed to suppress Sox9 activity, allowing cells to differentiate further.[6] In this line, mutations in WNT5a cause a skeletal brachydactylic phenotype in mice due to disrupted cell division and migration.[7,8] Even though both canonical and non-canonical Wnt signaling pathways are engaged in cartilage formation, most of the information regarding their role is based on the expression patterns of Wnt ligands or their antagonists in developing limbs.[9–13] Here, we aim to describe the functional contribution of Wnt ligands by preventing their secretion using Porcupine (PORCN) inhibitors.

PORCN encodes the endoplasmic reticulum membrane-bound O-acyltransferase,[14] which catalyzes the covalent attachment of a palmitoleate molecule (a monounsaturated fatty acid) to a conserved serine residue in Wnt proteins (commonly Ser209 in WNT3a), a highly specific post-translational modification essential for their secretion and functional maturation.[15,16] It is needed for the interaction of Wnt proteins with *Wntless*, which is responsible for transporting Wnt proteins from the Golgi apparatus to the cell membrane.[17] The attachment of palmitoleic acid makes Wnt proteins hydrophobic, which is crucial for their interaction with membranes and receptors, such as Frizzled (FZD), during signaling. No functionally redundant molecule for *Porcn* has been found in Drosophila, zebrafish, mice, or humans.[18–20]

The general functions of PORCN in musculoskeletal (MSK) tissues are primarily mediated through its essential role in Wnt signaling, which regulates a wide array of processes in bone, cartilage, and muscle development, as well as tissue homeostasis and regeneration.[18,21–24] As PORCN is essential for the secretion and activity of Wnt proteins, without PORCN,

Wnt secretion is impaired, leading to reduced activation of β-catenin and inhibition of osteogenesis. PORCN-mediated Wnt signaling is critical also for maintaining bone homeostasis, as seen in conditions like osteoporosis,[25] where aberrant Wnt signaling leads to impaired bone maturation and PORCN inhibition (using inhibitors like LGK974) reduces osteoblast differentiation and bone formation.[25,26] Moreover, proper chondrocyte maturation and cartilage formation also depend on a finely tuned Wnt signaling pathway. Therefore, dysregulated PORCN activity can result in skeletal disorders, such as osteoarthritis, where cartilage repair and homeostasis are disrupted.[27] Wnt signaling is important also for regulating the balance between muscle progenitor cell proliferation and differentiation. PORCN activity affects the secretion of Wnt proteins involved in muscle cell specification, but excessive canonical Wnt signaling impair myogenic differentiation, favoring other lineages like adipogenesis.[28] Hence, manipulating PORCN activity or Wnt secretion may be a potential therapeutic approach for bone repair, osteoporosis treatment, or cartilage regeneration.

In humans, mutations in the *PORCN* gene are associated with focal dermal hypoplasia (FDH) or Gorlin-Goltz syndrome, a rare dominant disorder characterized by pleiotropic symptoms, such as skeletal defects, skin issues, and abnormalities in ectodermal appendages. Limb malformations associated with this syndrome commonly include ectrodactyly, syndactyly, brachydactyly, or oligodactyly. Sometimes, there may also be a shortening or absence of long bones.[29–31] FDH predominantly affects females since the PORCN gene is located on the X chromosome. The absence of male offspring with this syndrome indicates that it may be embryonically lethal for them.[18] To date, over 100 different PORCN mutations causing FDH have been identified in humans. Most of these mutations result in loss of gene function due to small or large deletions and/or causing premature termination of protein synthesis.[32]

To investigate the role of PORCN in development, multiple mouse models were generated to specifically target PORCN function at different stages of embryogenesis. The complete loss of Porcn during early embryonic development results in lethality and is associated with severe morphological defects, including digit loss or fusion, limb truncation or shortening, and abnormalities in the body axis.[18,19,23] To study PORCN function more precisely in limb development, Porcn-floxed mice were crossed with transgenic mice expressing Cre recombinase under the control of limb-specific promoters, such as Prx1-Cre or Msx2-Cre. This approach allowed for the conditional deletion of Porcn within the developing limb ectoderm.[18,23] Male offspring from these crosses survived to term but exhibited profound limb malformations, including severe limb shortening and structural abnormalities. These findings highlight the critical role of PORCN in proper limb formation and provide valuable models for further investigating the molecular mechanisms underlying limb development.

Recently, several highly specific inhibitors of PORCN have been developed,[33] but no studies have been conducted to test their effects on cartilaginous tissue. Here, we analyzed the role of PORCN in chondrogenesis by altering its level using two synthetic small molecular inhibitors (C59 and LGK974). C59, a PORCN inhibitor, blocks the enzyme essential for the secretion and activity of Wnt ligands, effectively suppressing Wnt signaling.[34] This makes C59 a valuable tool for precisely downregulating Wnt activity and assessing its role in early chondrocyte differentiation and cartilage formation. Similarly, LGK974 inhibits PORCN by preventing the palmitoylation of Wnt ligands, a crucial modification required for their secretion and function,[35] allowing us to evaluate the effects of Wnt signaling suppression on chondrogenesis. In contrast, PF670462 selectively inhibits casein kinase 1δ/1ε (CK1δ/1ε), enzymes involved in multiple cellular processes, including Wnt signaling and circadian rhythm regulation.[36–39] CK1δ/1ε plays a critical role in the Wnt/β-catenin pathway, which is essential for chondrocyte differentiation.[36,40] By targeting distinct components of the Wnt signaling pathway, these inhibitors provide insights into its precise regulatory mechanisms in chondrogenesis. The use of small-molecule inhibitors also enables temporal control of signaling activity, which is particularly important given the dynamic and stage-specific roles of Wnt signaling during cartilage development.

We employed a range of model systems to investigate the impact of PORCN inhibitors on various stages of chondrogenesis, spanning from the initial mesenchymal condensation to the formation of hypertrophic cartilage. These models included both 2D and 3D cultures, as well as in vivo approaches, which allowed us to assess the effects of PORCN inhibition on chondrocyte differentiation in a comprehensive manner. Our findings consistently demonstrate that blocking PORCN can robustly stimulate chondrogenic differentiation, promoting the progression of mesenchymal cells towards chondrocytes. Additionally, we observed a significant increase in cartilaginous matrix production, indicating that PORCN inhibition not only accelerates the early stages of chondrogenesis but also supports the development of functional cartilage. This suggests that PORCN plays a crucial role in regulating the timing and progression of chondrocyte differentiation, and that its inhibition holds potential for enhancing cartilage formation at multiple stages of development.

## Materials and methods

### Embryonic material

Fertilized eggs from ISA Brown chickens were acquired from Integra Farm (Zabcice). Eggs were incubated in a humidified air incubator at 37.8 °C till they developed to stage HH20—3.5 d or HH26—4.5 to 5 d.[41] Two days before the experiment, approximately 2 mL of albumen was extracted from each egg to make handling the embryos easier. All experimental procedures with chicken eggs run under the license of the Animal facility at the Department of Experimental Biology, Faculty of Science, Masaryk University (MZE-45980/2023-13 143).

Zebrafish embryos were obtained from the Faculty of Science, Masaryk University. Larvae at the 5 d post-fertilization (dpf) stage were used for experiments and further analyses. Embryos were collected after natural spawning in breeding tanks of AB or SOX10:dsRed (ZFIN ID: ZDB-TGCONSTRCT-120523-6) zebrafish strains. After collection, embryos were kept in a standard E3 medium with daily medium changes. Animals were obtained and processed according to the rules established by the Laboratory Animal Science Committee of Masaryk University (MSMT-34667/2022-5).

Mice embryos collected at the E18 stage from the ICR strain (*Mus musculus var. alba*, *CD1*) were obtained from the Faculty of Medicine breeding facility at Masaryk University. Mice

were maintained at room temperature and under standard laboratory conditions with a 12-hr light and 12-hr dark cycle. All experimental procedures with mice embryos run under the license of the Animal facility at the Faculty of Medicine of Masaryk University (MZE-64131/2022-13 143).

## Micromass cultures

Primary mesenchymal cultures were established from the forelimb bud of HH20 chicken embryos. Forelimb buds were transferred into PSA solution (0.4 g KCl/L; 8 g NaCl/L; 0.35 g NaHCl3/L; 1 g glucose/L). Proteolytic tissue digestion was performed using Dispase II (10 U/mL; Sigma-Aldrich) at 37 °C in a thermostat, followed by the filtration of the cell suspension through a cell strainer (CLS431750-50EA, 40 $\mu$m, Sigma-Aldrich) to obtain a single cell population. $2 \times 10^7$ cells/mL were pipetted as 10 $\mu$L droplets in each well and left to adhere for 1 hr in the incubator before adding differentiating medium (40% Dulbecco's modified Eagle's medium—D6546-6X500ML, 60% Nutrient Mixture F-12 Ham—N6658-500ML; Sigma-Aldrich) with additions (10% FBS—F7524; 1% L-glutamine—G7513-100ML; 50 $\mu$g/mL ascorbic acid; 10 mM $\beta$-glycerol phosphate; 25 U/mL penicillin a 25 $\mu$g/ml streptomycin—P0781-100ML; Sigma-Aldrich), which was also used during processing of the cell suspension. Finally, the micromasses were cultured in an incubator at 37 °C with 5% $CO_2$ concentration for 3 or 6 d, with a change of differentiation medium every other day.

Selected concentrations (0.1, 0.3, 1, 5 and 10 $\mu$M) of the Wnt inhibitors—C59 (5148; Tocris Bioscience), LGK974 (S7143; Tocris Bioscience), or PF670462 (3316; Tocris Bioscience) dissolved in dimethyl sulfoxide (DMSO; 276855-250ML; Sigma Aldrich, Germany) were added to the medium. C59, LGK974, and PF670462 are selective small-molecule inhibitors that target the Wnt signaling pathway implicated in chondrogenesis. C59 (chemical Name: 4-(2-Methyl-4-pyridinyl)-*N*-[4-(3-pyridinyl)phenyl]benzeneacetamide) is a highly potent inhibitor of PORCN, a member of the MBOAT (membrane-bound O-acyltransferase) family with IC50 of 74 pM. Wnt-C59 effectively inhibits the processing of both canonical Wnt subtypes (1, 2, 3a, 6, 7b, 8a, 9a, 9b, 10) and non-canonical Wnt subtypes (4, 5a, 11, 16) (REF). LGK974 (WNT974, chemical name:

2-(2',3-dimethyl-[2,4'-bipyridin]-5-yl)-N-(5-(pyrazin-2-yl) pyridin-2-yl)acetamide) is highly specific PORCN inhibitor with an $IC_{50}$ of 0.1 nM.[35]

For experiments following the role of Wnt signaling, WNT3a (1324-WN-010; Bio-Techne) or WNT5a (645-WN-010; Bio-Techne) proteins were added to the medium at a concentration of 10 ng/mL either individually or in combination with LGK974.

Control micromasses were established and cultured with the appropriate amount of DMSO corresponding to the selected concentration required to dissolve Wnt inhibitors (Figure S2).

## Detection of early mesenchymal condensations and analysis of ECM production in micromasses

Three-day cultures of micromasses were fixed in 4% paraformaldehyde (PFA) after rinsing with PBS. Micromasses were transferred through descending methanol series (70%, 50%, 25%) and then rinsed in PBS with 0.1% Tween-20 (274348; Sigma-Aldrich). Samples were washed with blocking serum (BSA, 10% TWEEN, HISS, distilled $H_2O$) and, as a next step, incubated with rhodamine-conjugated peanut agglutinin (PNA) primary antibody (1:200; RL-1072-5, Vector Laboratories) overnight at 4 °C. PNA is a lectin that binds specifically to glycosylated structures present in the extracellular matrix (ECM), making it a valuable tool for assessing cartilage matrix composition and chondrogenic differentiation. As this antibody selectively binds to the surface of condensing chondroprogenitor cells,[2] it was used to visualize the early stages of cartilage development. Furthermore, micromasses were washed with PBS and photographed with a Leica S6D camera (Leica Micro-system, Germany).

After 1, 3, or 6 d of culture, the micromasses were rinsed with PBS and then fixed in 4% PFA. Subsequently, they were washed with PBS and then with 0.1 M HCl. Finally, fixed cultures were stained at least overnight with 0.5% Alcian blue in HCl at room temperature. The samples were incubated in Alcian blue until sufficiently saturated, followed by washing with 70% ethanol. In each experiment, the number of micromasses was standardized, with at least 5 spots photographed and evaluated per condition. Each repetition included control micromasses for comparison, and all repetitions were stained for the same duration of time. While some variation in staining intensity may exist between repetitions, each individual repetition was always consistent. Stained micromasses were photographed using a microscope with a Leica S6D camera (Leica Microsystem). For further evaluation, the pixel count per area was analyzed using Photoshop CC 2017 (Adobe System Incorporated).

Finally, some micromasses were stained with hematoxylin (C0303; Diapath S.p.A.) on days 1, 3, or 6 of culture to visualize the size of the individual condensation nodules.

## RNA isolation and reverse transcription

To analyze differences in the expression of selected genes during chondrogenesis after treatment with Wnt inhibitors, we established micromass cultures from limb buds of HH20 chicken embryos. The micromasses were cultured with the corresponding Wnt inhibitors for 3 or 6 d. Subsequently, the micromasses were lysed by RLT lysis buffer (74 106; Qiagen) with beta-mercaptoethanol (10 $\mu$L/1 mL; M3148-100ML; Sigma-Aldrich). RNA was isolated using the Mini RNeasy kit (74106; Qiagen), followed by transcription of the RNA into complementary DNA (cDNA) using the gb Reverse Transcription Kit (3020; Biotech) in a Mastercycler Pro Thermal Cyclers (Eppendorf). The concentration and purity of RNA and cDNA were verified spectrophotometrically with a NanoDrop 1000 instrument (Thermo Fisher Scientific).

## Gene expression analyses using qPCR

The cDNA obtained from micromasses cultivated for 1, 3, or 6 d were used for the analyses of the gene expressing while using qPCR with commercially available primer sets and TaqMan fluorophore-labeled probes designed by Thermo Fisher. The probes used for analysis were *Sox9* (Gg03364395_m1; mesenchymal condensations) and *Col2a1* (Gg03365340_m1; structural protein of cartilage) as early markers of differentiating chondrocytes. *Ihh* (Gg03815062_s1; prehypertrophic chondrocytes) and *Gli1* (Gg03320038_m1; transcriptional effector of the HH signaling pathway) were used as indicators of progression to intermediate stages of chondrogenesis. *Mmp9* (Gg03338322_g1) or *Mmp13* (Gg07161833_m1; both expressed in hypertrophic chondrocyte) and *Oc3* (Gg03326527_m1; osteoid zone) were used as markers for the late stages of chondrogenesis. *CCND1* (Gg03339845_m1)

was used as a marker of cell proliferation, and *Axin2* (Gg03365745_m1) as an evaluator of inhibition of canonical Wnt signaling. The expression of analyzed genes was normalized by the $2^{-\Delta\Delta Ct}$ method against the expression of *Hprt1* (Gg03338900_m1), which was used as a housekeeping gene. cDNA from samples was mixed with Ideal Master mix (3007; Generi Biotech), and the protocol for PCR with TaqMan probes had reaction conditions of 95 °C/600 s for the preincubation and amplification step with 95 °C/15 s/50 cycles and 62 °C/60 s.

Micromasses cultivated for 1, 3, or 6 d were analyzed by SYBR Green PCR to detect changes in *PORCN* expression during development. Sequences of chicken primers used for SYBR Green analysis: *PORCN* forward primer—TGC ACC CAT CGC AAT AAG GA, *PORCN* reverse primer—CCC CCA AAT AGG ACA GGT GG; *HPRT1* forward primer—TTG TTG GAT ACG CCC TCG AC, *HPRT1* reverse primer—TCC CCG TCT CAC TGA TCA CA. The gene expression of each sample was expressed in terms of the threshold cycle and normalized by the $2^{-\Delta\Delta Ct}$ method against the expression of *HPRT1*. cDNA from samples was mixed with SG Master mix (3005; Generi Biotech), and the protocol for PCR using SYBR Green was as follows—an initial preincubation step at 95 °C for 10 min, afterward 45 denaturation cycles at 95 °C for 10 s, then annealing at 51 °C for 10 s and an extension at 72 °C for 10 s, followed by melting and cooling. All steps above from TaqMan and SYBR Green PCR were performed on a LightCycler 96 (Roche). For both types of PCR analyses, four spots were seeded in each well, four wells were analyzed as biological replicates per cultivated conditions, and each sample was run in three technical replicates in each qPCR reaction.

## Establishment of chondrogenic organoids

The limb buds were processed like micromasses from chicken embryos at the HH26 stage. Cells were seeded at a concentration of $2 \times 10^7$ cells/mL onto the culture dish lid in 20 $\mu$L hanging drops, in which they gradually condensed into organoids. After 24 hr, the differentiation medium (40% Dulbecco's modified Eagle's medium—D6546-6X500ML, 60% Nutrient Mixture F-12 Ham—N6658-500ML; Sigma-Aldrich) with additions (10% FBS—F7524; 1% L-glutamine—G7513-100ML; 50 $\mu$g/mL ascorbic acid; 10 mM $\beta$-glycerol phosphate; 25 U/mL penicillin and 25 $\mu$g/ml streptomycin—P0781-100ML; Sigma-Aldrich) was replaced, and 1 $\mu$M LGK974 was added to the media of half the organoids. Organoids were cultured for 14 d in the incubator at 37 °C with 5% $CO_2$ concentration and medium changes daily.

Microwell platform for chondrogenic organoids was designed in CleWin 5 software (WieWeb Software) and developed using master molds created by MicroWriter ML3 (Durham Magneto Optics Ltd.). Molds were fabricated from a clean $5 \times 5$ cm Borosilicate glass (B-2-04-18; Nanofilm) coated with two layers of SU-82100 (Y131273 0500L; Micro Resist Technology GmbH) to obtain a depth of 400 $\mu$m according to a previous publication.[42] The mold was then covered by PDMS Sylgard 184 (1673921; Dow Corning Corporation), mixed from the base and curing agent at 10:1, and degassed under vacuum for 20 min. The molds with PDMS were cured on a hot plate for 2 hr at 80 °C. The final circular shape of the platforms was obtained by punching PDMS with a 6 mm puncher. The PDMS microwell platforms were then sterilized by heat and manually anchored to 48-well plates. The platforms were coated with 0.2% Pluronic F-127 (P2443-250G; Sigma-Aldrich) to prevent cell adhesion, degassed under vacuum for 20 min, and washed many times with 1x PBS. The $2 \times 10^7$ cells/mL cell suspension was placed in 30 $\mu$L drops on the surface of the microwell and transferred to the incubator for 60 min. Then, the platform was covered with 300 $\mu$L of differentiation media with a single cell suspension and cultivated for 14 d in the incubator at 37 °C with 5% $CO_2$ concentration. 1 $\mu$M LGK974 was added to the media of half the organoids, and the medium was changed every 2 d.

The microwell platform for chondrogenic organoids was designed in CleWin 5 software (WieWeb Software) and developed using master molds created by MicroWriter ML3 (Durham Magneto Optics Ltd.) (more details in Supplementary Methods). Then, the platform was covered with 300 $\mu$L of differentiation media with a single cell suspension and cultivated for 14 d. 1 $\mu$M LGK974 was added to the media of half the organoids, and the medium was changed every 2 d.

After collection, the organoids were fixed in 4% PFA, washed with running water, dehydrated in ascending alcohol series (30%, 50%, 70%, 80%, 85%, 90%, 95%, and 100%), transferred to xylene and embedded in paraffin. Paraffin blocks were cut into 5 $\mu$m sections using a Leica RM2145 rotary microtome. Cartilaginous tissue was detected on organoid sections by staining with Alcian blue (1016470500; Sigma-Aldrich) and visualizing nuclei using nuclear stain (N3020-100ML; Sigma-Aldrich). For size evaluation, the number of pixels per area was analyzed using Photoshop CC 2017 (Adobe System Incorporated). Diameter analysis of organoids cultivated on microwell platforms was performed in ImageJ (NIH).

## Tibia cultures

Mouse tibias were dissected from embryos at the E18 stage. The cleaned tibiae were placed in culture dishes on metal grids and immersed in differentiation medium (40% DMEM—Dulbecco's modified Eagle's medium, 60% Nutrient Mixture F-12 Ham; Sigma-Aldrich) with additions (10% FBS—F7524; 1% L-glutamine; 50 $\mu$g/mL ascorbic acid; 10 mM $\beta$-glycerol phosphate; 25 U/mL penicillin and 25 $\mu$g/mL streptomycin; Sigma-Aldrich). Tibiae were cultivated for 8 d in the incubator at 37 °C, with a 5% $CO_2$ concentration and medium changes daily. Three culture dishes with mouse tibiae were established in every experiment, one as control and others with added Wnt inhibitor (C59, LGK974, PF670462) at 0.5 and 1 $\mu$M concentrations.

Tibiae were fixed in 4% PFA, and subsequent decalcification was performed using 10% EDTA. Tibiae were rinsed with water before being transferred to 70% ethanol. They were further dehydrated by ascending alcohol series (80%, 95%, and 100% EtOH), transferred to xylene, and embedded in paraffin. The blocks of embedded tibiae were cut into 5 $\mu$m sections using a Leica RM2145 rotary microtome. Mayer's H&E staining was used for histological analysis.

Bone length measurements were consistently performed from the proximal to the distal condyle at two time points: once at the beginning of the first day and again at the conclusion of the eighth day of the experiment. These measurements were conducted using Axiovision Rel. 4.8 (Zeiss Microscopy) imaging software to ensure accuracy and reproducibility. This approach allowed for precise quantification

of bone growth over the experimental period, facilitating comparisons between different experimental conditions.

### Immunohistochemical analysis of protein expression

For immunohistochemical analysis, sections of developing limbs, tibiae, or organoids were transferred to the glass slide and placed in a thermostat at 56 °C for 30 or 60 min. It was followed by deparaffinization of the sections and their hydration with a descending alcohol series. Antigen retrieval was performed at 97 °C in DAKO (S2367; Dako Targeted Retrieval Solution, pH 9) or citrate solution (pH 6). Eliminating nonspecific binding was achieved by applying blocking serum for 30 min at RT. Primary antibodies used for signal detection: anti-PORCN antibody (1:100, ab105543; Abcam) on tibial and limb sections, anti-$Na^+/K^+$-ATPase (1:100, ab76020-100 $\mu$L; Abcam) on organoid samples. Alexa fluorophore-labeled secondary antibody fluor 488 (1:200, A-11008; Thermo Fisher) was applied for signal visualization. Next, the sections were rinsed in PBS and mounted using the histological mounting medium—Fluoroshield with 4′,6-diamidino-2-phenylindole (DAPI) (F6059, Sigma-Aldrich) to visualize cell nuclei. Fluorescence images were taken using a Leica DM LB2 fluorescence microscope (Leica Microsystems). The cell area was evaluated using ImageJ (NIH). Following numbers of pictures were taken: limbs—46 photos, tibiae—30 photos, and organoids—52 photos.

### Gene expression analyses by RNAscope

Tibial sections were used for gene expression analyses using the RNAscope method (Advanced Cell Diagnostics). Tibial sections were first fixed on a glass slide at 56 °C and then deparaffinized and rinsed in 100% ethanol. Next, hydrogen peroxide (322335; Advanced Cell Diagnostics) was added to the sections. After boiling samples in a particular buffer at 100 °C, protease (322331; Advanced Cell Diagnostics) was applied. A probe containing the complementary sequence of the gene selected for detection, *Collagen type 10a1* (*Col10a1*; 426181; Advanced Cell Diagnostics) or *Ptch1* (402818; Advanced Cell Diagnostics), was applied to the prepared tissue. The Ptch1 probe was utilized as a marker for the proliferating zone, while *Col10a1* served as a marker for the hypertrophic zone.[43,44] Both probes were employed to assess and visualize differences in the width of these zones between tibiae treated with PORCN inhibitors and those cultured in control medium. This analysis allowed for a comparative evaluation of how PORCN inhibition influences the organization and expansion of growth plate zones.

After probe hybridization for two hours, amplification and subsequent labeling with Cy3 fluorochrome—TSA Plus Cyanine 3 kit (1:1000, NEL744001KT; PerkinElmer) was performed. Finally, the nuclei were visualized using DAPI (323108; Advanced Cell Diagnostics) and mounted with a coverslip using ProLong Gold Antifade Mountant (P10144; Thermo Fisher Scientific). The RNAscope Multiplex Fluorescent v2 kit (323110; Advanced Cell Diagnostics) was used for all steps of the RNAscope procedure.

Fluorescence images were taken with a Leica DM LB2 fluorescence microscope (Leica Microsystems) and merged in Photoshop CC 2017 (Adobe System Incorporated).

### Effect of Wnt inhibitors on zebrafish embryo

Embryos were cultured in E3 medium (34.8 g NaCl; 1.6 g KCl; 5.8 g $CaCl_2{\cdot}2H_2O$; 9.78 g $MgCl_2{\cdot}6H_2O$), stock of 60x E3 media was diluted to 1x and 100 $\mu$L of 1% methylene blue (M9140, Sigma-Aldrich) was added to 1 L of media. After 12 or 24 hr, LGK974, C59, or DMSO was added to the media, and embryos were cultivated until 5 d post-fertilization (dpf) with daily medium changes. In the control group, DMSO was dissolved in the medium to eliminate its possible toxic effect on fish development. After five days, larvae were fixed in 4% PFA or methanol and stored at 4 °C. Samples were dehydrated by ascending alcohol series, transferred to xylene, and embedded in paraffin. Subsequently, the blocks were cut into 5 $\mu$m sections using a Leica RM2145 microtome. For morphological analysis, sections were stained with H&E and Alcian blue (1016470500; Sigma-Aldrich). Alternatively, SOX10:DsRED animals were washed in PBS 2 hr after fixation in 4% PFA. Using SOX10:DsRED zebrafish provided us a valuable tool for studying processes during chondrogenesis due to the specific role of SOX10 and the advantages of the DsRED fluorescent reporter. During cartilage development, SOX10 drives the early stages of chondrocyte differentiation by activating SOX9, another essential chondrogenic transcription factor. By labeling SOX10-expressing cells, we could track the early stages of chondrocyte lineage specification. DsRED is a red fluorescent protein that allows live imaging and visualization of SOX10-expressing cells under a fluorescence microscope.

Animals were then embedded in 1% TopVision low melting point agarose (R0801; Thermo Fisher Scientific) on a glass-bottom dish and imaged as a whole mount using a Leica SP8 confocal microscope. Confocal Z-stack images were captured, and the resulting image series was imported into Imaris software (version 10.2, Bitplane). Three-dimensional reconstructions were then generated and presented as videos (Video S1, S2, and S3) or as a snapshot (Figure 8D). Imaris software was subsequently used to measure the length of the palatoquadrate cartilage.

### Statistical analysis and evaluation

Statistical analyses were performed in GraphPad Prism 8 using a two-sample Student's *t*-test (used at least partially in every analysis except Figure 3D and 5C); when data had inhomogeneous variances, Welch's *t*-test was used (Figure 1C and D, 2D, 3C, 4B, 5B´´ and B´´´, and 7B). Among the statistical tests, one-way ANOVA followed by post hoc analysis using Fisher's LSD test was also used (Figure 3D). Results that did not follow a normal distribution tested by the Shapiro–Wilk test were evaluated using the non-parametric Mann–Whitney test (Figure 1D, 4B, 5C, 6B, and 7B). Details of the specific tests used for each analysis are provided in the respective figures along with the data.

## Results

### PORCN expression decreases with the progression of chondrogenesis

PORCN has been previously found to be expressed in several tissues,[15] however, its expression pattern and role in developing cartilage have not been reported. Here, we first analyzed PORCN protein expression across different stages of cartilage development in the limb of mice embryos (Figures 1A

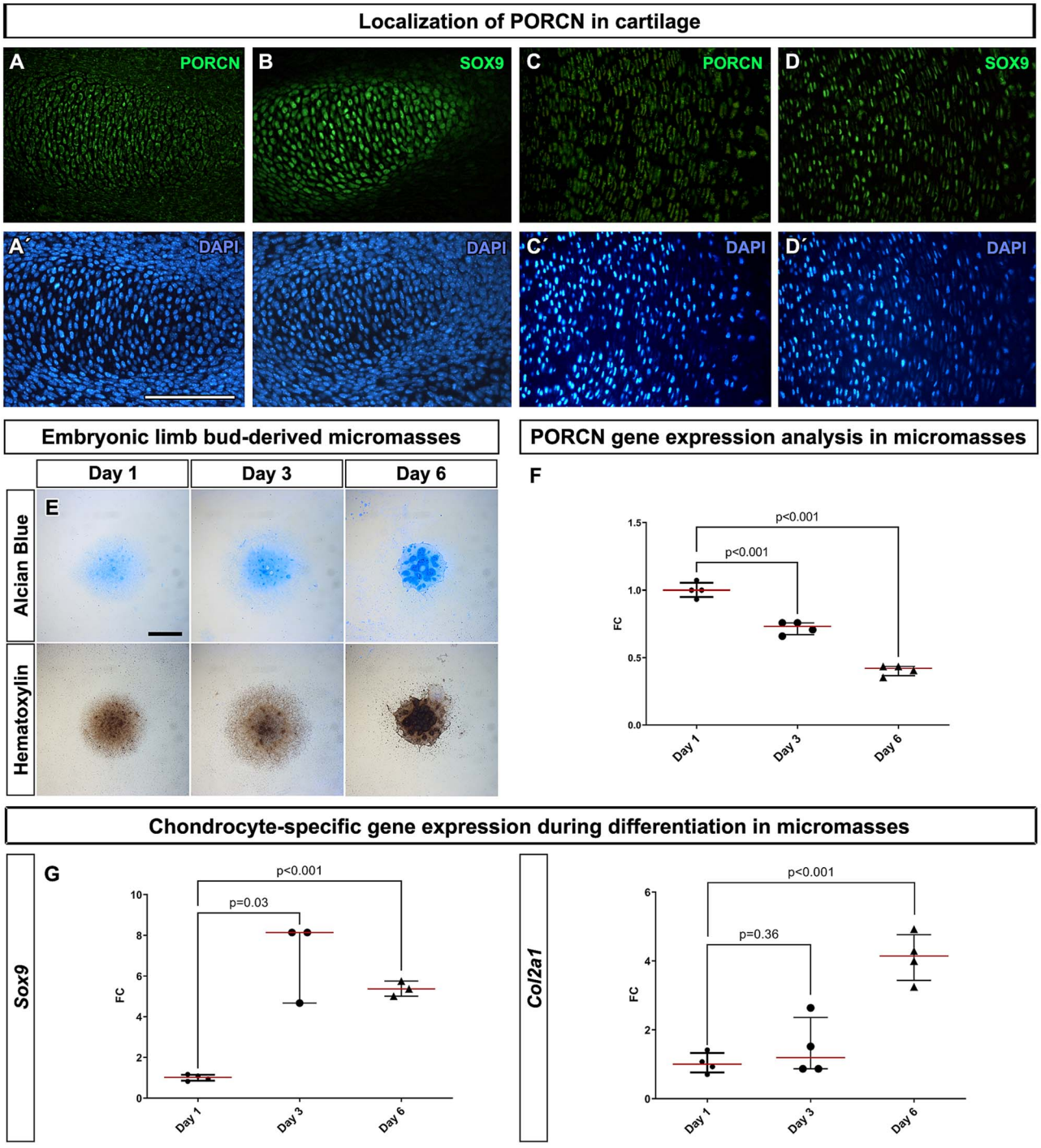


**Figure 1.** PORCN expression during endochondral ossification in limbs and early chondrogenesis in micromasses. (A-D) PORCN and Sox9 expression detected in differentiated chondrocytes by immunohistochemistry. (A, B) PORCN signal was located in Sox9-positive cells during early endochondral ossification as observed at E13.5 of mice hindlimb. (C, D) Later at E18, weaker PORCN signal was observed in proliferating and prehypertrophic zone in the tibia growth plate while Sox9 expression was still strong. Nuclei are counterstained by DAPI. Scale bar = 100 $\mu$m. (E) Micromass cultures established from chicken forelimb buds (stage HH20) cultivated for 1, 3, and 6 d. Alcian blue staining uncovered the production of ECM from day 3 with the progression of its deposition at day 6. Small cartilaginous nodules were produced and observed from day 1 when visualized by hematoxylin staining. Scale bar = 1 mm. (F) *PORCN* expression analyzed by qPCR uncovered the highest expression in 1-d cultures and significantly decreased in micromasses cultivated for 3 and 6 d. (G) At the same time points, *Sox9* and *Col2a1* were evaluated to determine progress of chondrogenesis in micromass cultures. Gene expression was evaluated as a relative expression to *Hprt1* gene expression (housekeeping). Four spots were seeded in each well, four wells were analyzed as biological replicates per cultivated conditions and each sample was run in 3 technical replicates in each qPCR reaction. Data are displayed as FC as the ratio to gene expression on day 1. Two-tailed Student's *t*-test or Welch's *t*-test was used for the statistical analyses performed on samples from three independent experiments (see Supplementary material for other repetitions). Abbreviations: ECM, extracellular matrix; FC, fold changes; PORCN, Porcupine.

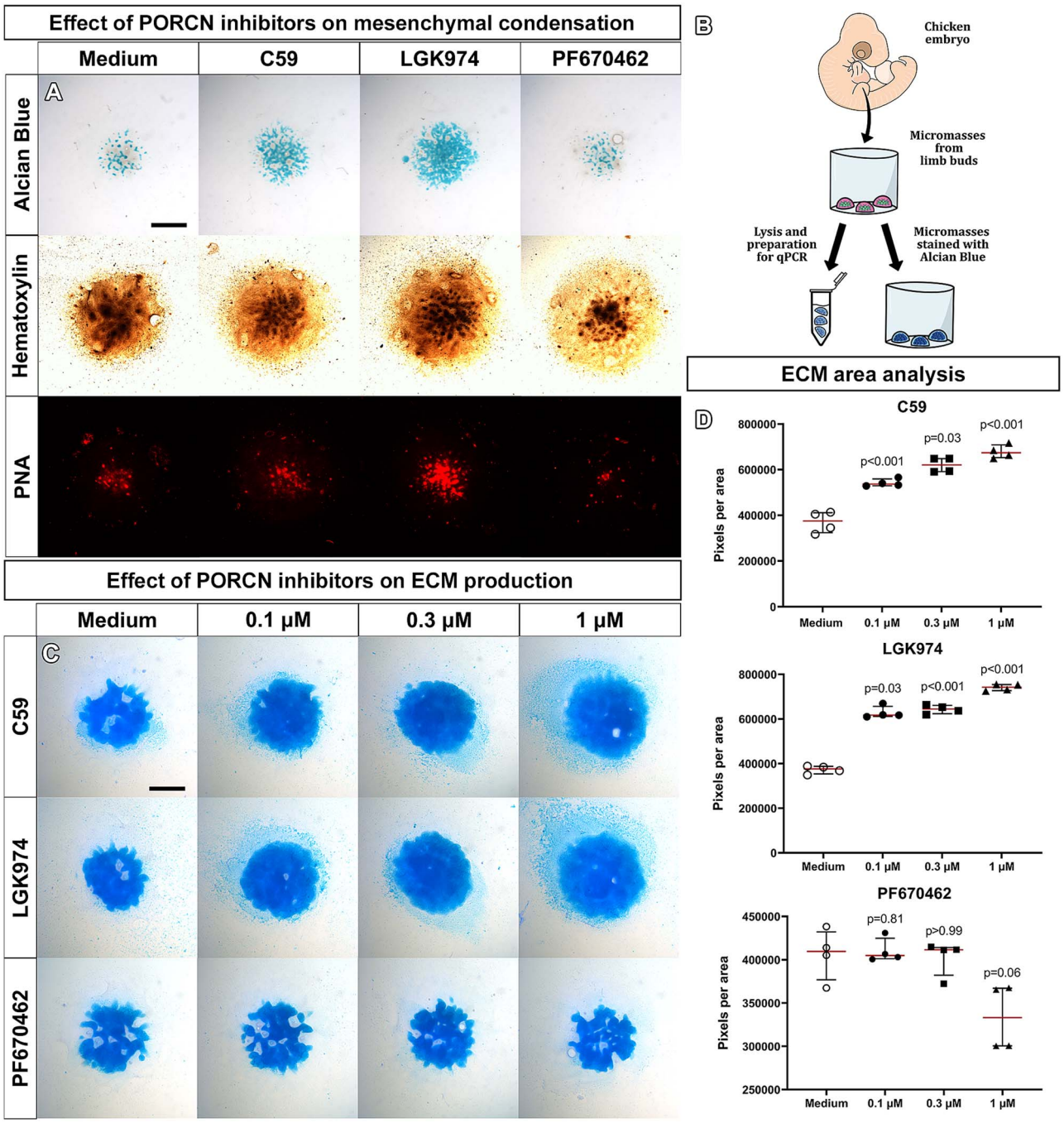


**Figure 2.** Effect of PORCN inhibitors on mesenchymal condensation formation and production of cartilaginous ECM. (A) Micromass cultures established from chicken forelimb buds (stage HH20) were cultivated for 3 d to evaluate the effect of Wnt inhibitors on early chondrogenesis. Alcian blue, hematoxylin, and rhodamine-conjugated PNA staining revealed an increased amount of cartilaginous nodules after C59 and LGK974 treatment. In contrast, the treatment with PF670462 reduced the amount of cartilaginous nodules (1 $\mu$M concentration of inhibitors was used). Scale bar = 1 mm. (B) Schema of experimental design. Micromasses were established from chicken forelimb buds (stage HH20) and were collected for gene expression analyses evaluated by qPCR or stained for the assessment of ECM production. (C) Micromass cultures established from chicken forelimb buds (stage HH20) cultivated for 6 d. Production of the ECM was evaluated using Alcian blue staining. An increased amount of ECM was produced after C59 and LGK974 treatment, while a low production level was observed after the PF670462 application. Three different concentrations of inhibitors were used (0.1 $\mu$M, 0.3 $\mu$M, or 1 $\mu$M), and progression in ECM production was observed with increased concentrations of PORCN inhibitors. Scale bar = 1 mm. (D) Graphs displaying analyses of blue pixels in Alcian blue stained micromasses treated with individual Wnt inhibitors after 6-d cultivations. Data is shown as a number of blue pixels. Two-tailed Student's *t*-test or Welch's *t*-test was used for statistical analyses ($n = 4$; spots evaluated per cultivated conditions) performed on samples from three independent experiments (see Supplementary material for other repetitions). Abbrevations: ECM, extracellular matrix; PNA, peanut agglutinin; PORCN, Porcupine.

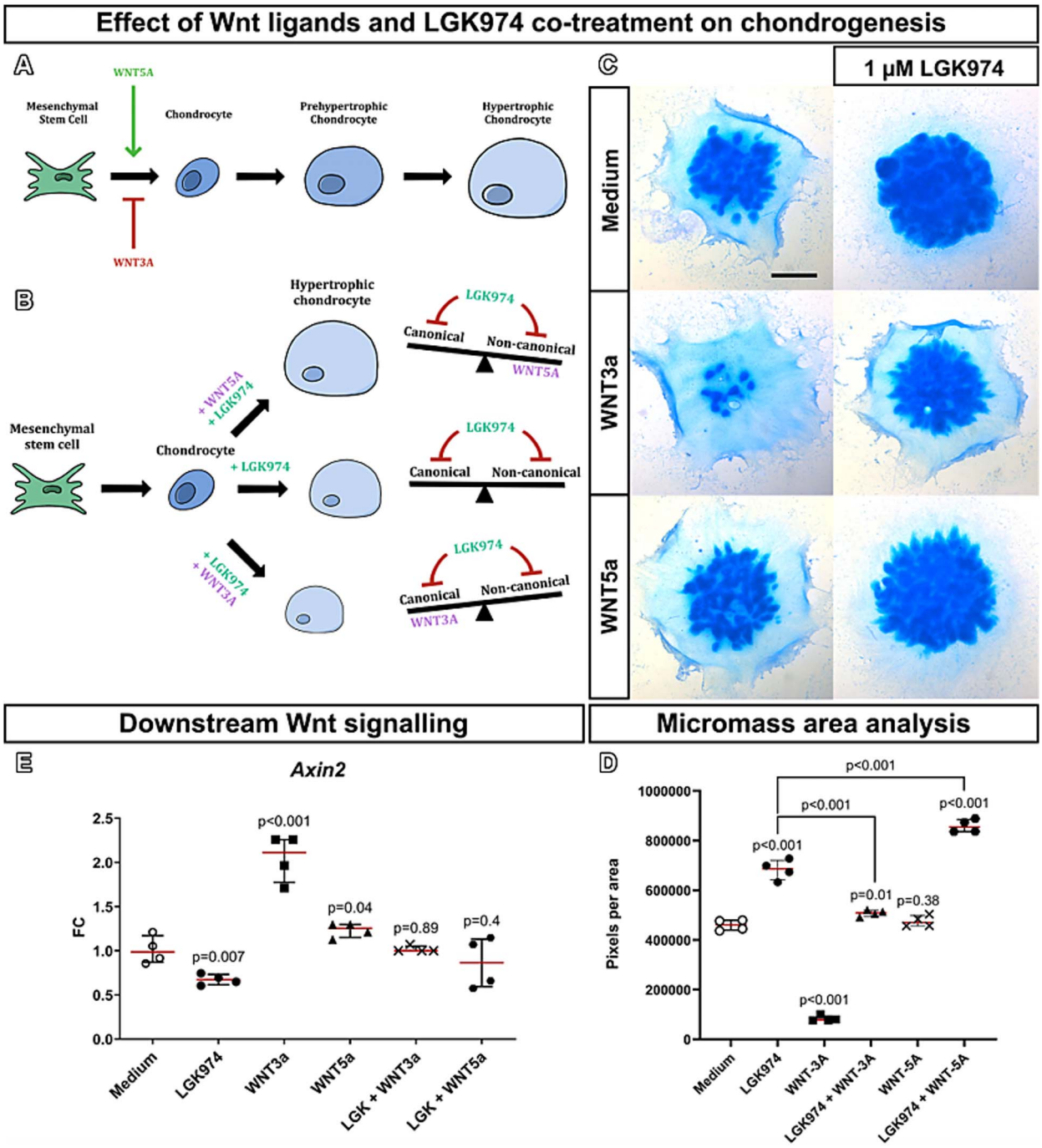


**Figure 3.** Impact of PORCN inhibition while simultaneously activating canonical or non-canonical Wnt pathway on chondrogenesis. (A) Schema of individual differentiation steps of chondrocytes evaluated during the study together with the general effect of WNTs on early chondrogenesis, where non-canonical signaling enhances differentiation of chondrocytes towards hypertrophy while canonical signaling behaves antagonistically and maintains cells in non-differentiated mesenchymal status. (B) Schema of experimental design and summary of results in challenging simultaneously canonical and non-canonical signaling in the mesenchymal cells. PORCN inhibitor LGK974 was applied on cells alone or in combination with WNT5a or WNT3a to evaluate the effect of PORCN inhibition on both signaling pathways. (C) ECM production was evaluated on micromasses established from chicken forelimb buds (stage HH20) that were cultivated with 1 $\mu$M LGK974 in combination with WNT3a (10 ng/mL) or WNT5a (10 ng/mL) for 6 d. Application of LGK974 rescued WNT3a inhibitory effect on chondrogenesis and enhanced ECM production in WNT5a treated cultures. Scale bar = 1 mm. (D) Graphs displaying the analyses of blue pixels in Alcian blue stained micromasses after 6 d of cultivation. A decreased amount of ECM was observed after WNT3a treatment, and the addition of LGK974 restored its production. WNT5a did not affect ECM production, and its level was comparable to control cultures. Simultaneous treatment of WNT5a and LGK974 significantly increased the amount of ECM. Data is displayed as a number of blue pixels. One-way ANOVA followed by post hoc analysis using Fisher's LSD test was used for statistical analyses ($n = 4$; spots evaluated per cultivated conditions) performed on samples from three independent experiments (see Supplementary material for other repetitions). (E) Graphs of *Axin2* expression analyses of micromass cultures after 6-d cultivations evaluated by qPCR. Four spots were seeded in each well, four wells were analyzed as biological replicates per cultivated conditions and each sample was run in three technical replicates in each qPCR reaction. The level of *Axin2* expression was related to *Hprt1* gene expression, and FC as the ratio to control micromasses are displayed in individual treatments. Two-tailed Student's *t*-test or Welch's *t*-test was used for statistical analyses performed on samples from three independent experiments (see Supplementary material for other repetitions). Abbreviations: ECM, extracellular matrix; FC, fold changes; PORCN, Porcupine.

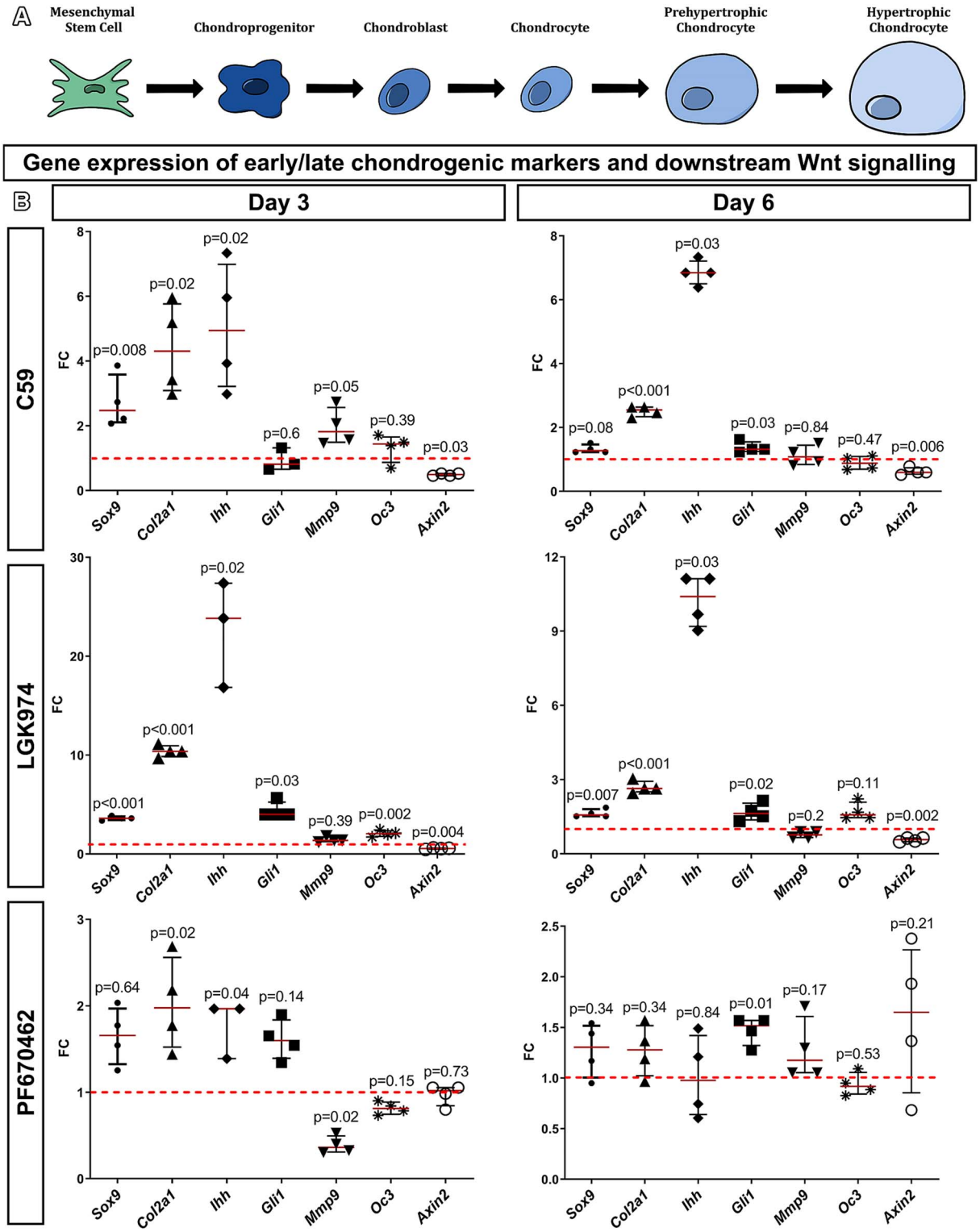


**Figure 4.** Gene expression analyses of chondrogenic markers in micromass cultures. (A) Schema of individual chondrocyte differentiation steps evaluated by qPCR. (B) Graphs of gene expression analyses of micromass cultures after 3 and 6 d of cultivations by qPCR. Inhibitors of PORCN (C59, LGK974) significantly enhanced the expression of *Sox9* and *Col2a1* already after 3 days' cultivation, and *Col2a1* expression remained escalated even after 6 d of cultivation. *Ihh* expression was increased at both time points when using any PORCN inhibitor, while *Gli1* was only elevated in 6-d cultures. There were differences in the level of *Gli1* expression between PORCN inhibitors in 3-d cultures, and only LGK974 displayed statistically significant upregulation. The expression of *Mmp9* was increased in 3 d of cultivated micromasses after C59 treatment and *Oc3* in 3 d of cultivated micromasses after LGK974 treatment. The expression of *Axin2* was downregulated after treatment with PORCN inhibitors at both time points. On the other hand, PF670462 treatment caused insignificant changes in most of the analyzed genes except for *Col2a1* upregulation or *Mmp9* downregulation at 3-d cultures and increased expression of *Ihh* at both analyzed stages. The gene of interest expression level was related to *Hprt1* gene expression, and FC as ratio to control micromasses are shown on graphs. Two-tailed Student's *t*-test, Welch's *t*-test or Mann–Whitney test was used for statistical analyses performed on samples from three independent experiments (refer to the Supplementary material for 2 additional repetitions of the experiments). Abbrevations: FC, fold changes; PORCN, Porcupine.

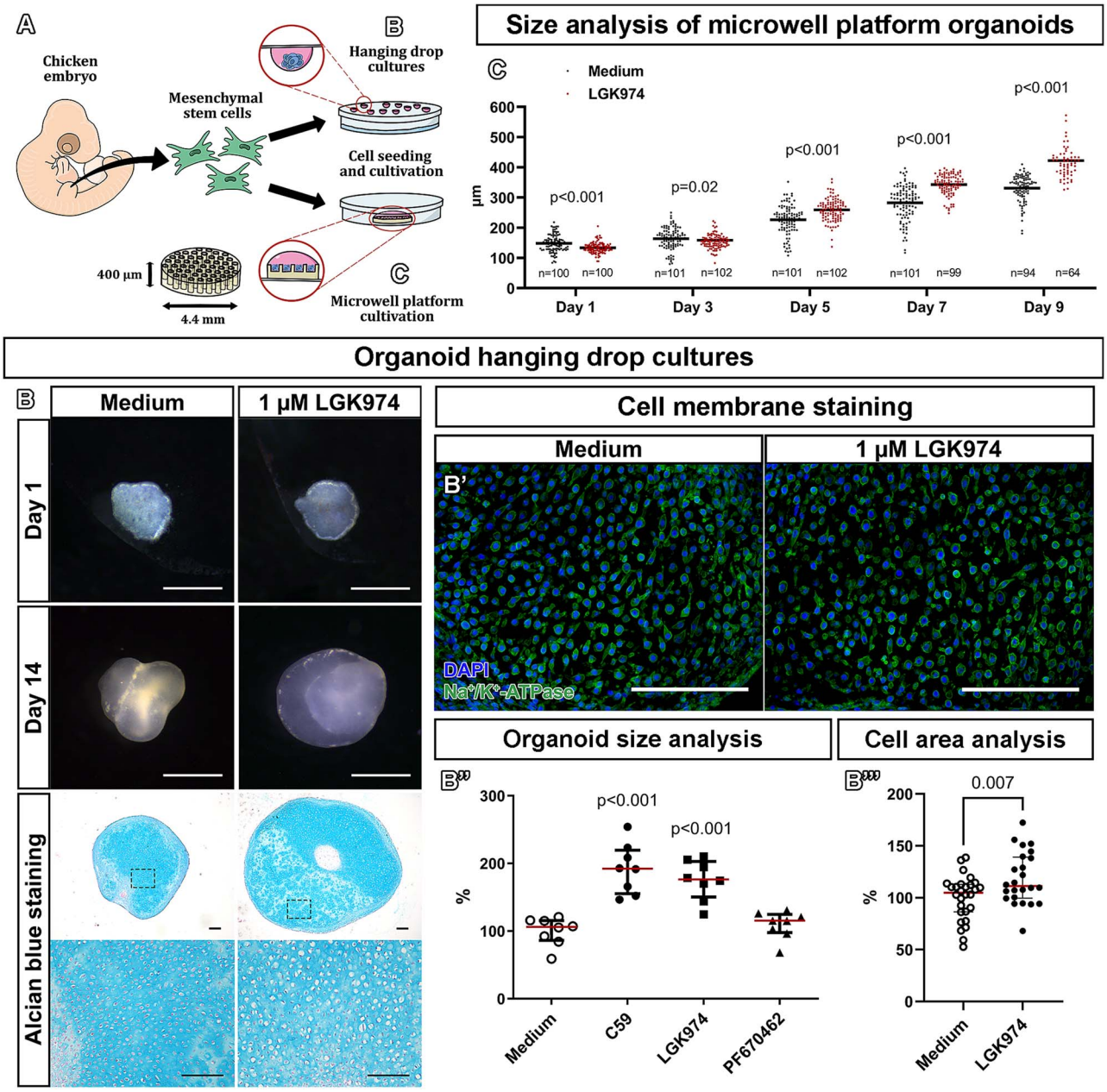


**Figure 5.** The effect of PORCN inhibitors on the growth of cartilaginous 3D cultures. (A) Schema of experimental design of 3D cultures. The mesenchymal cells separated from chicken embryonic limbs (stage HH26) were seeded as hanging drops or in PDMS microwell platforms. (B) LGK974 treatment (1 $\mu$M) increased the size of 3D hanging drop cultures following 14 d of cultivation. Microscopic sections stained by Alcian blue exhibit enlargement of organoids as well as hypertrophic chondrocytes. Scale bars: macroscopic view = 1 mm, sections = 100 $\mu$m. (B´) Immunohistochemistry labeling of cytoplasmatic membranes by $Na^+/K^+$-ATPase to visualize cell outlines. Scale bar = 100 $\mu$m. (B´´) graphs displaying organoids cultured with Wnt inhibitors for 11 d, where C59 (1 $\mu$M) or LGK974 (1 $\mu$M) treatment exhibited increased size of organoids, while PF670462 (1 $\mu$M) treatment did not significantly change their size. Data are displayed as the number of pixels of the organoid area in Wnt inhibitor-treated samples relative to the size of organoids cultivated in medium ($n = 8$; organoids evaluated per cultivated conditions). Two-tailed Student's *t*-test or Welch's *t*-test was used for the statistical analyses. (B´´´) Cell area analyzed in ImageJ using $Na^+/K^+$-ATPase labeled cells cultivated as hanging drops. LGK974 (1 $\mu$M) treated cultures exhibited statistically significant enlargement of the cell surface compared to cells grown in the medium. The data represent the cell area (in $\mu m^2$) of PORCN inhibitor-treated samples relative to the cell area of organoids grown exclusively in the medium ($n = 20$; cells evaluated per cultivated conditions). Two-tailed Student's *t*-test or Welch's *t*-test was used for the statistical analyses performed on samples from three independent experiments (refer to the Supplementary material for 2 additional repetitions of the experiments). Abbrevation: PORCN, Porcupine.

and A´, S1). At E13.5, cartilage templates in hindlimbs displayed numerous proliferating cells and a distinct population of differentiated, enlarged SOX9-positive chondrocytes (Figure 1B and B´). PORCN was detected in differentiating chondrocytes of the central area of the cartilage, while the surrounding perichondrium was negative (Figures 1A and S1). At E14.5, proliferating chondrocytes at the edges of cartilage still expressed a high level of PORCN, and the signal was located especially close to the nuclei, while cells near the center of each growing cartilaginous element withdrawn from the cell cycle and underwent the process of hypertrophic differentiation were PORCN-negative (Figure S1). Next, we

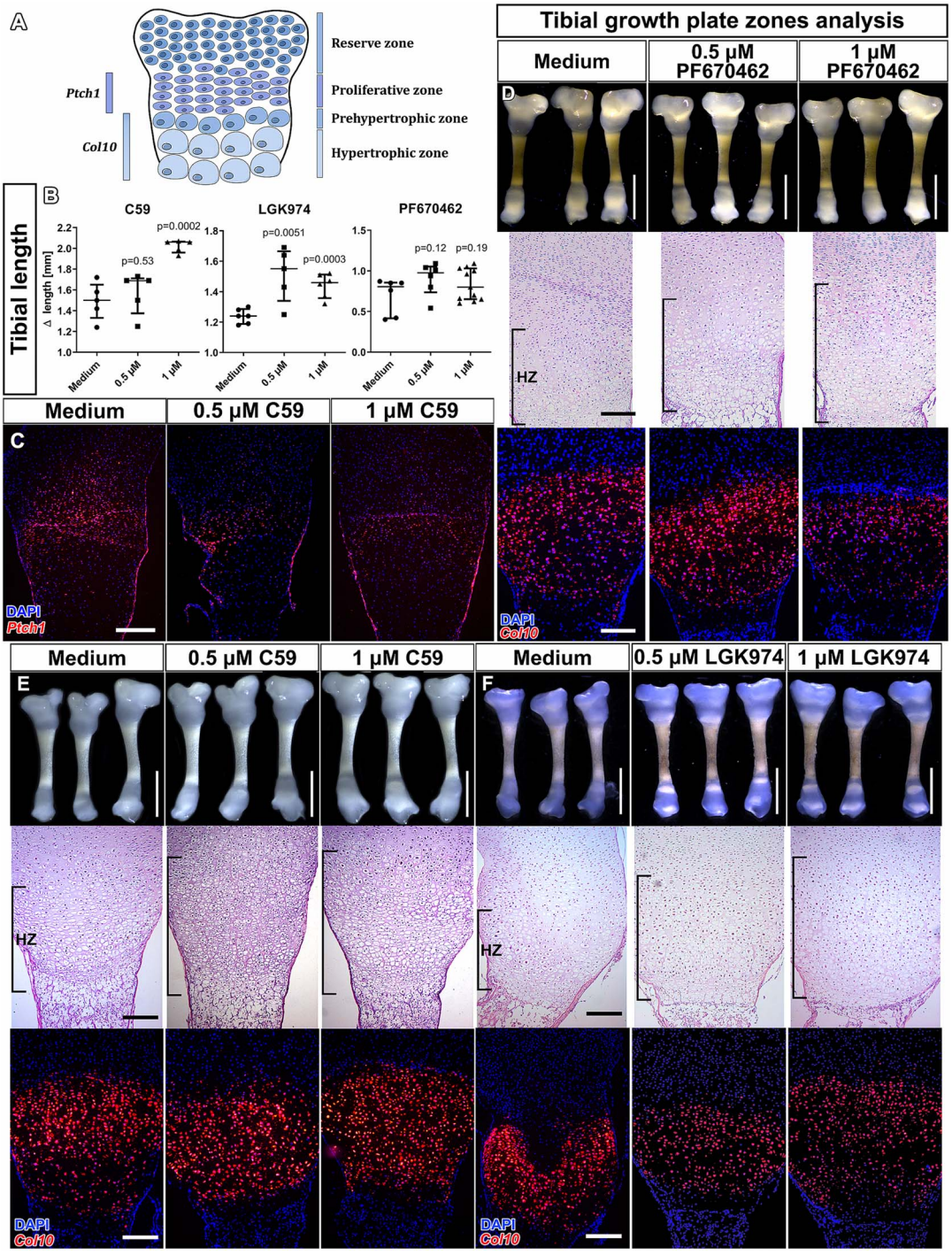


**Figure 6.** PORCN inhibitors alter endochondral ossification in tibias. Tibias isolated from E18 mouse embryos were cultured with Wnt inhibitors (C59, LGK974, PF670462) at concentrations of 0.5 or 1 $\mu$M. (A) Schema of individual zones during endochondral ossification and their markers selected for further analyses. (B) Differences in tibia length before and after 8 d of cultivation (data are displayed as subtraction of initial length from final bone length). At least 4 tibias were evaluated for each experimental condition. Two-tailed Student's *t*-test or Mann–Whitney was used for the statistical analyses performed on samples from 3 independent experiments (see Supplementary material for other repetitions). (C) Expression of *Ptch1* (marker of proliferating zone) detected on histological sections of cultivated tibias by RNAscope. The treatment with C59 (0.5 or 1 $\mu$M) downregulated *Ptch1* expression in the tibia growth plate. Scale bar = 100 $\mu$m. (D) The overall appearance of tibias treated with PF670462 at the end of the experiment, where the shown tibias are representatives selected from 1 independent experiment after 8 d of cultivation. Histological sections stained by H&E reveal an increase in the hypertrophic zone (HZ) and a decrease of *collagen type 10a1* (a marker of the HZ, DAPI counterstain nuclei). Scale bar = 100 $\mu$m. (E) The overall appearance of tibias treated with C59 at the end of the experiment. C59 treatment elongated tibias with a more considerable difference observed when using 1 $\mu$M concentration after 8 d of cultivation. An expanded HZ was observed on histological sections stained by H&E even at the lowest-used concentration (0.5 $\mu$M) of C59. *Col10a1* (DAPI counterstain nuclei) expression slightly increased in tibias treated with C59 inhibitor. Scale bar = 100 $\mu$m. (F) Overall appearance of the tibia treated by LGK974 at the end of the experiment. LGK974 treatment noticeably elongated cultured tibias after 8 d of cultivation, especially when using 1 $\mu$M concentration. An expanded HZ was visible on histological sections stained with H&E at both analyzed concentrations. An increase of *Col10a* (red signal, DAPI counterstain nuclei) expression was observed in tibias treated with LGK974 inhibitor. Scale bar = 100 $\mu$m. Abbrevation: PORCN, Porcupine.

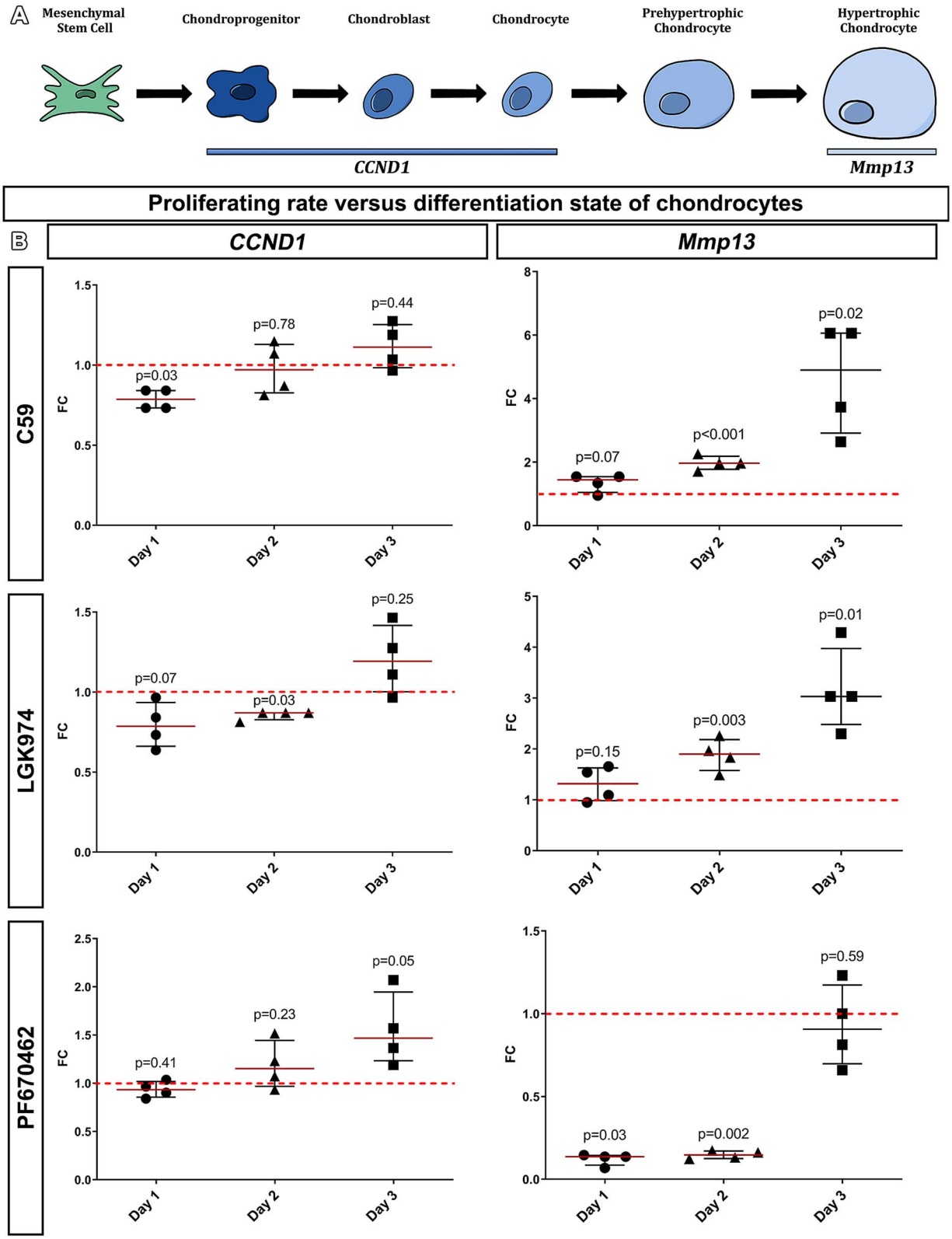


**Figure 7.** Determination of PORCN inhibitor's effect on cell proliferation versus differentiation in early stages of cultivation. (A) Schema of individual chondrocyte differentiation steps in micromass cultures evaluated by qPCR. (B) Graphs of gene expression analyses of micromass cultures established from chicken limb buds (stage HH20) after 1, 2, and 3 d of cultivations, which were evaluated by qPCR. The level of *CCND1* expression was reduced in the 1-d or 2-d cultivations with both PORCN inhibitors—C59 and LGK974 (1 $\mu$M), with no change observed in the expression at 3 d compared to control cultures. *Mmp13* expression was significantly increased in 2-d micromass cultures after PORCN inhibition, and this trend was even more evident in 3-d micromasses. The gene of interest expression level was related to *Hprt1* gene expression, and FC as ratio to control micromasses are shown on graphs. Two-tailed Student's *t*-test, Welch's *t*-test or Mann–Whitney test was used for statistical analyses performed on samples from three independent experiments (refer to the Supplementary material for 2 additional repetitions of the experiments). Abbrevations: FC, fold changes; PORCN, Porcupine.

investigated the expression of PORCN protein in the tibial growth plate of E18 mice to explore its role in the later stages of chondrocyte differentiation when ECM surrounding hypertrophic cells mineralizes and ultimately chondrocytes undergo apoptosis. The highest signal of PORCN was again observed prominently in the proliferating and prehypertrophic areas of the growth plate in contrast to the low signal in the hypertrophic mineralized zone (Figures 1C and D, S1).

To further quantify *Porcn* gene expression during chondrocyte differentiation, we established primary mesenchymal cell cultures derived from limb buds of HH20-stage chicken embryos (Figure 2E). These densely seeded cell cultures, called micromasses, provide a three-dimensional environment that allows cell–cell interactions resembling conditions during chondrogenesis in embryos.[45]

Micromasses were cultured for up to 6 d, allowing us to track different stages of chondrocyte differentiation in vitro.[46] By day 3, the formation of cartilaginous nodules was clearly visible in differentiation medium, as demonstrated by hematoxylin staining (Figure 1E). Alcian blue staining revealed the early stages of ECM production in these 3-d-old micromasses (Figure 1E), while extensive ECM deposition was observed by day 6. Gene expression analysis showed that *Porcn* levels were highest in 1-d-old cultures and significantly decreased in micromasses maintained for 3 and 6 d (Figures 1F and S3). Furthermore, we observed a significant increase in *Sox9* and *Col2a1* expression in both 3-d-old and 6-d-old micromasses (Figures 1G and S4) similar to *Ihh* and *Mmp9* (Figure S5). This upregulation indicates that chondrocyte differentiation was already underway at the earlier analyzed stage. *Sox9*, a key transcription factor for chondrogenesis, was used because it plays a crucial role in initiating and maintaining chondrocyte differentiation,[47] while *Col2a1*, a major component of the cartilage ECM, serves as a marker of mature chondrocytes.[48] The progressive increase in their expression suggests an active transition from mesenchymal condensation to cartilage matrix production, reinforcing the successful progression of chondrocyte differentiation within our micromass culture system.

Based on these observations, we summarize that PORCN expression is located in the developing cartilage and it was detected in differentiating chondrocytes. However, the level of PORCN expression is reduced with the progression of chondrogenesis.

## PORCN inhibitors enhanced the formation of early mesenchymal condensation

To investigate the role of PORCN in early chondrogenesis, we treated micromass cultures with two well-characterized PORCN inhibitors, C59 and LGK974, for 3 d (Figure 2A and B). Then, we assessed chondrocyte differentiation by evaluating the formation of condensation centers and ECM production. These condensation centers, also referred to as cartilage nodules, are clusters of densely packed mesenchymal cells that serve as precursors to cartilage. This condensation process is a critical early step in chondrogenic differentiation, leading to the subsequent formation of cartilage tissue.[49] Hematoxylin staining showed a significant increase in nodule labeling in cultures treated with PORCN inhibitors (C59 or LGK974, 1 $\mu$M), indicating that PORCN inhibition may promote mesenchymal cell condensation and potentially impact the early stages of cartilage development (Figures 2A, S6, and S7), while diameter of micromasses was smaller (Figure S7). In contrast, condensation centers of micromasses cultured with the inhibitor of casein kinase 1 (1 $\mu$M PF670462), which can also block Wnt pathway, were not affected or difference was smaller (Figure 2A and S7). To evaluate the presence of condensing chondroprogenitors demonstrating induction of condensations centers, we performed rhodamine-conjugated PNA staining, where PNA is a lectin that selectively binds to the surface of condensing chondroprogenitor cells.[50] This staining confirmed an earlier onset of chondrocyte differentiation and a higher amount of condensation centers following treatment with C59 and LGK974 (Figure 2A) but not with PF670462 (Figure 2A).

## PORCN inhibitors augmented the production of extracellular matrix in micromasses

To examine the impact of PORCN inhibitors on chondrogenesis during later stages, micromasses were cultured for six days, allowing for the progression of ECM production (Figures 2C and D, S8, S9, and S10). At this stage, the ECM had developed extensively, and individual mesenchymal condensations were no longer distinguishable. To quantify ECM production, we analyzed the total area (in pixels) stained by Alcian blue, a marker of sulfated glycosaminoglycans, which are essential components of cartilage matrix (Figures 2C and D, S9, and S10).

Treatment with C59 and LGK974 (both PORCN inhibitors) enhanced ECM production in a dose-dependent manner (Figure 2C and D). However, at concentrations exceeding 5 $\mu$M, C59 led to a reduction in ECM production, likely due to cytotoxic effects, as evidenced by decreased staining intensity (Figures S9 and S10). In contrast, LGK974 did not exhibit toxicity, even at higher concentrations, suggesting a more favorable safety profile for prolonged chondrogenesis studies (Figures S9 and S10). Additionally, treatment with PF670462, a CK1$\delta$/1$\varepsilon$ inhibitor, did not enhance ECM production (Figure 2C and D). This suggests that PORCN inhibition specifically enhances chondrogenesis through mechanisms independent of CK1$\delta$/1$\varepsilon$ signaling.

## Synergistic regulation of chondrogenesis by canonical Wnt inhibition and non-canonical activation

Next, we assessed the expression levels of *Axin2*, a well-established Wnt signaling target and reporter gene,[51] in micromasses following Wnt inhibitor treatment. Micromasses derived from HH20-stage chicken limb bud mesenchyme were cultured with 1 $\mu$M of C59, LGK974, or PF670462 for 3 or 6 d. Treatment with both PORCN inhibitors (C59 and LGK974) led to a significant reduction in *Axin2* expression at both mRNA and protein levels (Figures 3E and S8). In contrast, inhibition of CK1$\delta$/1$\varepsilon$ with PF670462 did not result in a significant change in *Axin2* expression (Figure S8). These findings indicate that PORCN inhibition effectively suppresses endogenous Wnt/$\beta$-catenin signaling in micromass cultures, whereas CK1$\delta$/1$\varepsilon$ inhibition does not have the same impact, further highlighting the specific role of PORCN in regulating Wnt-dependent chondrogenesis.

Since PORCN inhibition prevents the secretion of both canonical and non-canonical Wnt ligands,[16,52] we aimed to further investigate its interaction with these pathways. Previous studies have shown that different Wnt signaling pathways

exert opposing effects on chondrogenesis. While canonical Wnt/$\beta$-catenin signaling inhibits mesenchymal cell differentiation,[3] non-canonical Wnt signaling promotes chondrogenesis by facilitating chondrocyte differentiation (Figure 3A).[53] For our analysis, we specifically selected WNT3a (a key activator of canonical Wnt signaling) and WNT5a (a major regulator of non-canonical Wnt signaling) to examine their roles in chondrogenesis under PORCN inhibition.[53]

We treated micromass cultures with Wnt ligands (10 ng/mL) either individually or in combination with LGK974 to assess their effects on chondrogenesis. WNT3a alone inhibited chondrogenesis, but co-treatment with LGK974 rescued nodule formation and ECM production, restoring chondrogenic activity (Figures 3B-D, S11, and S12).

In contrast, WNT5a alone induced a mild increase in chondrogenesis. However, when combined with LGK974, there was a dramatic expansion in micromass size (Figure 3B-D). This enlargement surpassed even the level of ECM production observed in micromasses treated with LGK974 alone, indicating a strong synergistic effect between PORCN inhibition and WNT5a in promoting chondrogenesis (Figure 3B-D and S13).

In summary, these findings suggest that Wnt/$\beta$-catenin signaling actively suppresses chondrocyte differentiation and ECM production in micromass cultures. This inhibitory effect can be effectively counteracted by PORCN inhibition, which blocks the secretion of Wnt ligands. On the other hand, while non-canonical WNT5a signaling clearly supports chondrogenesis, its activity appears to play a limited role in micromass differentiation. The strongest enhancement of chondrogenesis was achieved when canonical WNT3a signaling was inhibited via PORCN blockade, while non-canonical Wnt signaling was actively stimulated by exogenous WNT5a, highlighting a synergistic interaction between these pathways in promoting cartilage formation.

## PORCN inhibition accelerated chondrocyte differentiation

To gain deeper insight into the molecular mechanisms by which PORCN inhibitors accelerate chondrocyte hypertrophy, we analyzed gene expression changes associated with both early (3-d micromass cultures) and late (6-d micromass cultures) stages of hypertrophic differentiation. By utilizing micromass cultures, we were able to examine these stages separately, allowing for a more precise evaluation of the temporal effects of PORCN inhibition on chondrocyte maturation.

Our analysis revealed that PORCN inhibitors significantly upregulated the expression of *Sox9* (Figures 4B, S14, and S15), a key transcription factor essential for early chondrogenesis, which is expressed in mesenchymal condensations.[54] Additionally, *Col2a1*, encoding the primary structural protein of cartilage, was also strongly induced.[48] This effect was evident in micromasses treated with C59 and LGK974 after three days of culture, with *Col2a1* expression remaining elevated through day 6 (Figures 4B, S14, and S15). These findings suggest that PORCN inhibition enhances both early chondrocyte commitment and sustained cartilage matrix production.

Furthermore, micromasses treated with PORCN inhibitors for 3 and 6 d exhibited a significant upregulation of *Ihh* expression (Figures 4B, S14, and S15), a key marker of prehypertrophic chondrocytes.[55] This suggests that PORCN inhibition promotes the transition from proliferating chondrocytes to the prehypertrophic stage, a critical step in cartilage maturation and endochondral ossification.

To further investigate whether PORCN inhibitors strongly activate the Hedgehog (HH) pathway, we examined the expression of *Gli1*, a key transcriptional effector of HH signaling.[56] LGK974 treatment led to a significant increase in *Gli1* expression at both time points, while C59-treated micromasses showed a similar increase only after 6 d of cultivation. This delayed response in C59-treated cultures corresponds to a less pronounced effect of this inhibitor on ECM production, in contrast to the more robust impact observed with LGK974 (Figures 4B, S14, and S15).

To assess the impact of PORCN inhibitors on the later stages of hypertrophic chondrocyte differentiation, we analyzed the expression of matrix metalloproteinase 9 (*Mmp9*) and osteocalcin-like protein 3 (*Oc3*). Mmp9 is highly expressed in late mineralized hypertrophic cartilage just before osteoclast invasion,[57] but we observed minimal changes in its expression following PORCN inhibitor treatment at both analyzed time points (Figures 4B, S14, and S15). Similarly, only slight changes were detected in *Oc3* expression, a marker of the osteoid zone during endochondral ossification (Figures 4B, S14, and S15).[58] Notably, a small reduction in *Mmp9* expression was observed in 3-d-old micromass cultures treated with PF670462, although no effect on *Oc3* expression was seen (Figures 4B, S14, and S15).

These findings suggest that PORCN inhibitors primarily accelerate chondrocyte differentiation by enhancing the early stages of chondrogenesis, rather than promoting the later processes involved in hypertrophic cartilage maturation.

## PORCN inhibitors induced the growth of cartilaginous organoids and increased the size of their chondrocytes

Next, we utilized cartilaginous organoids as they better mimic the physiological microenvironment of cartilage compared to 2D cultures, and can replicate key tissue functions such as ECM production in a 3D context. These characteristics make organoids valuable in vitro models for studying developmental processes, disease modeling, drug testing, and tissue engineering.[59–61] To investigate the effects of PORCN inhibitors in a 3D system, we optimized protocols for generating cartilage organoids from embryonic chicken limb tissues using two distinct approaches (Figures 5A, S16, and S17).

For the first approach, we employed a traditional hanging drop system. Mesenchymal cells isolated from chicken embryonic limbs were seeded in 20 $\mu$L drops on the lid of a culture dish at a concentration of $2 \times 10^7$ cells/mL and left to cultivate for 14 d. Cultures derived from HH20 and HH26 embryonic stages formed 3D condensates overnight. HH20-derived organoids exhibited rapid growth but were less compact and eventually disintegrated during cultivation (data not shown). In contrast, cultures established from the later HH26 stage formed compact 3D structures that remained tightly attached throughout the entire cultivation period. Based on these observations, we selected the HH26 stage cultures for further analysis of the effects of PORCN inhibitors.

Organoids treated with PORCN inhibitors (C59 and LGK974) for 14 d exhibited a noticeable increase in cartilage mass compared to those cultured in standard differentiation media without inhibitors (Figures 5B, B´´, and C, S16, and S19). In contrast, treatment with PF670462 did not significantly affect the size of the organoids (Figures 5B´´ and S16). These findings in 3D cultures corroborate our previous observations from 2D micromass cultures (Figure 2),

further highlighting the positive effect of PORCN inhibitors on chondrogenesis.

Moreover, histological analysis and Alcian blue staining (Figures 5B, S16, and S18) revealed increased ECM production and the presence of larger chondrocytes after treatment with LGK974, supporting the accelerated onset of chondrocyte differentiation observed earlier in the micromass cultures (Figures 2, 4, and S16).

We also developed miniaturized PDMS microwell platforms as a solution to facilitate the cultivation of cartilage organoids and enable extensive screenings within a single experiment (Figure S17). A single-cell suspension (30 $\mu$L) was placed on each of the 64 microwell platforms and cultivated for 9 d. Organoids treated with the PORCN inhibitor LGK974 showed an increased cartilage mass compared to those cultured in standard differentiation media (Figures 5C and S17). Analysis of different time points revealed that the cultures initially shrank during the early stages of cultivation (day 1 and day 3) as cell condensation began. From day 5, a significant increase in size was observed, with a more prominent enlargement in the LGK974-treated cultures (Figure 5C).

To further investigate changes in cell size, we labeled organoid sections with anti-$Na^+/K^+$-ATPase (Figures 5B´ and S20), which stains the cell membranes,[62] allowing us to analyze cell area using ImageJ. Cell surface measurements were performed manually by analyzing 20 randomly selected cells from each cultivation condition. Chondrocytes from organoids generated by the hanging drop method and treated with LGK974 exhibited a statistically significant increase in cell surface area compared to those cultured in standard media (Figure 5B´ and B´´´).

In summary, PORCN inhibitors significantly promoted cartilage mass and cell enlargement in cartilage organoids, particularly when treated with LGK974. These findings support the notion that PORCN inhibition accelerates early stages of chondrogenesis and chondrocyte differentiation in a 3D culture system, offering a promising model for further exploration of cartilage development.

## Treatment with PORCN inhibitors elongated tibiae by stimulating cartilage hypertrophy

To assess whether the effects of C59, LGK974, and PF670462 are similar in the growth plate during endochondral bone formation, we established tibia organ cultures from E18 mouse embryos. Dissected bones were cultured for 8 d, and we compared the effects of 2 different concentrations of Wnt inhibitors on tibia elongation. Treatment with 1 $\mu$M C59 and LGK974 significantly increased the size of the tibia cartilage, while PF670462 had no effect on tibia length, which remained similar to the control (Figures 6B, D-F, and S21).

Histological analysis revealed that the extension of tibiae treated with PORCN inhibitors was caused by the expansion of the prehypertrophic and hypertrophic zone in the growth plate (Figures 6E, F and S23). This finding was supported by detection of *Col10a1* expression in tibias, commonly used as a marker for prehypertrophic and hypertrophic chondrocytes.[43,44] The RNAscope analyses uncovered increased expression of *Col10a1* in tibias treated with C59 and LGK974, confirming the expansion of the hypertrophic zone (Figure 6E and F). The treatment with PORCN inhibitors caused such a high increase of *Col10a1* expression in the hypertrophic zone of the distal growth plate that there was observed the fusion of the growth plate to hypertrophic chondrocytes near the articular surface (Figure S22). These chondrocytes will eventually participate in the formation of a secondary ossification center.[63] On the other hand, the cultivating tibiae with PF670462 caused only small changes in the structure of individual growth plate zones (Figures 6D and S23).

Therefore, PORCN inhibitors were confirmed to increase the size of the tibiae by expanding the prehypertrophic and hypertrophic zones of the growth plate. This result might seem contradictory, as these zones are generally associated with the later stages of cartilage differentiation. Moreover, we previously showed that PORCN inhibition primarily accelerates the early stages of chondrogenesis, such as ECM production and chondrocyte differentiation, with minimal effects on later hypertrophic stages, including *Mmp9* and *Oc3* expression in 6-day micromass cultures. This raises the question of how inhibitors that primarily influence early differentiation stages could lead to the expansion of the hypertrophic zones. The observed expansion of the prehypertrophic and hypertrophic zones in the growth plate in response to PORCN inhibitors could be explained by several mechanisms. These may involve both the acceleration of chondrogenesis and a shift in the timing of hypertrophic differentiation.

PORCN inhibitors might promote early chondrogenesis by enhancing ECM production and chondrocyte differentiation in the earlier stages of cartilage formation. This increased early differentiation could lead to a larger pool of chondrocytes entering the prehypertrophic and hypertrophic stages more quickly than normal. Thus, the expansion of these zones may be a result of a faster progression of cells through the differentiation stages. Moreover, PORCN inhibition might affect the dynamic balance between proliferation, differentiation, and hypertrophic maturation in the growth plate. The increased ECM production and cell proliferation in early stages could create a push toward hypertrophic differentiation in the later stages, leading to an overall larger cartilage mass in the growth plate. Indeed, the treatment with PORCN inhibitors led to a reduction in the size of the proliferative zone and a downregulation of *Ptch1* expression, a well-known marker of this zone (Figure 6C).[44] *Ptch1* is typically expressed in proliferating chondrocytes, where it plays a crucial role in regulating the response to HH signaling, which is essential for maintaining the balance between proliferation and differentiation.[43] The observed reduction in *Ptch1* expression suggests that PORCN inhibition may not only impact the early stages of chondrogenesis but also influence the transition of chondrocytes through the proliferative phase of cartilage development. This may shift the focus of differentiation more quickly toward the prehypertrophic and hypertrophic stages, where cartilage matrix production and cellular enlargement are prominent, potentially explaining the expansion of the later zones observed in the growth plate.

To further confirm cellular processes behind observed morphological changes in tibias, we further quantify the expression of *CCND1* as a marker of cell proliferation[64] and *Mmp13* as a marker for hypertrophy in early micromass cultures,[65] which allowed us to follow individual early steps of chondrocyte differentiation separately. In agreement with our previous observations in tibias, *Mmp13* expression was significantly increased in 2-d micromass cultures, and this trend was even more evident in 72-hr-old micromasses (Figures 7B, S24, and S25). On the other hand, *CCND1* exhibited reduced

expression in the 1-d or 2-d cultivations with no observed change in the expression at 3 d compared to control micromasses (Figures 7B, S24, and S25).

These findings highlight a complex interplay between Wnt signaling, HH signaling, and cartilage differentiation, suggesting that PORCN inhibitors may accelerate the overall chondrocyte differentiation process by modulating the timing and progression through various stages of cartilage development.

### PORCN inhibitors shortened the zebrafish body axis and thickened craniofacial cartilages

To evaluate the impact of PORCN inhibitors in vivo, we utilized zebrafish as an ideal model to study their effects on early development, including chondrogenesis. Embryos were exposed to C59, LGK974, or a solvent at different time points (0-, 12-, or 24-hr post-fertilization, hpf) (Figure 8A and S26).

Embryos treated with C59 or LGK974 at 0 hpf exhibited a significant reduction in body length, near-complete loss of caudal structures, and abnormal cranial patterning (Figure 8, S26, S27, and S28). Early inhibition resulted in varying degrees of developmental abnormalities, with the most common being a shortened longitudinal body axis and edema, particularly at higher concentrations of the PORCN inhibitors (Figure S26). To specifically investigate the effects of PORCN inhibition on chondrogenesis in zebrafish, we administered the inhibitors also at later developmental stages, namely 12 and 24 hpf. As expected, the phenotypic effects were milder with later inhibitor exposure, though the shortening of the body axis remained evident even in zebrafish treated with LGK974 at 24 hpf (Figure 8B). The reduction in body length was dose-dependent, whereas in previous studies shortening occurred upon PORCN inhibition, without addressing concentration dependency.[20] In the control group, zebrafish exposed to media containing DMSO showed no developmental changes up to the collection time at 5 d post-fertilization (dpf) (Figure 8B).

Staining of the skeleton with Alcian blue revealed that craniofacial cartilages became shorter and thicker after C59 treatment (Figure S27, S28, and S29). The same result was observed in transgenic Sox10:DsRed zebrafish cultivated with C59 or LGK974, which we used to visualize arrangement of chondrocytes in craniofacial cartilages (Figure 8C). Chondrocytes in inhibitor-treated zebrafish were less polarized and displayed a more rounded or cuboidal phenotype, in contrast to the cylindrical morphology observed in controls (Figure 8C—palatoquadrate and Meckel's cartilage). This lack of polarity likely affected the overall length of the palatoquadrate, which was significantly shorter in LGK974-treated embryos (Figure 8C and D, Supplementary Video S1, S2 and S3). Next, we assessed the width of the palatoquadrate and found a significant increase in its size (Figure 8D). Similarly, the number of chondrocytes was increased in Meckel's cartilage following LGK974 treatment (Figure 8D).

In summary, the observed increase in palatoquadrate width appears to result from altered growth direction, likely due to tissue disorganization and disrupted structural patterning. This effect may be attributed to the preferential targeting of the non-canonical Wnt signaling pathway, which is known to play a more prominent role in craniofacial development. Given that non-canonical signaling is particularly active in the head region, PORCN inhibition may have led to dysregulated chondrogenesis and aberrant expansion of craniofacial cartilage structures.

## Discussion

During chondrogenesis, the Wnt signaling pathway is one of the essential regulatory mechanisms affecting chondrocyte proliferation, differentiation and ECM production, as well as cartilage replacement by bone tissue.[66] Several Wnt ligands, which play crucial roles in chondrogenesis in limb or craniofacial development. Non-canonical Wnt signaling ($\beta$-catenin independent) generally promotes chondrogenesis and plays a key role in regulating cytoskeletal organization, cell migration, and differentiation.[1,53] These pathways, including the Wnt/PCP and Wnt/$Ca^{2+}$ pathways, are crucial for supporting cartilage formation. For example, WNT5a facilitates chondrogenic condensation and differentiation.[6,11,67] WNT5A regulates the transition of chondrocytes from the resting to the proliferative zone and also their maturation into hypertrophic cells.[6] It is suggested that WNT5A suppresses SOX9 activity, allowing the cells to further differentiate. WNT5b, similar to WNT5a, supports cartilage formation by activating the Wnt/PCP pathway, contributing to chondrogenesis.[6,11,67] Similarly, WNT11 regulates mesenchymal condensation and chondrocyte differentiation by influencing cell polarity and migration, playing a key role in cartilage formation.[53,67] Early chondrogenesis is promoted by WNT4, though its effects can vary depending on the cellular context, influencing how cells respond to chondrogenic signals.[11,53,67,68] On the other hand, canonical Wnt signaling ($\beta$-catenin dependent) generally acts as an inhibitor of chondrogenesis.[1] This pathway helps prevent premature cartilage formation by maintaining cells in a proliferative state and inhibiting SOX9, the key regulator of chondrogenesis.[47,53,54] For instance, WNT3a strongly activates $\beta$-catenin signaling, which in turn suppresses chondrocyte differentiation.[3,69] Increased WNT3a activity leads to a reduction in *Sox9* expression and *collagen type II* (*Col2a1*), both of which are crucial for early cartilage formation, thus inhibiting the onset of chondrogenesis.[3] Similarly, WNT9a (formerly WNT14) has a dual role: while it inhibits early chondrogenesis, it is also essential for joint formation.[53,70] WNT9a promotes the development of the joint interzone by restricting chondrogenic differentiation in specific regions, ensuring the proper formation of joints.[12]

Any dysregulation or imbalance in these processes leads to malformations or skeletal defects.[1,66] Such skeletal abnormalities, including shortened or completely missing long bones, have been described in patients with FDH caused by mutations in the PORCN.[18,21,23,29–31] One treatment strategy for diseases with aberrant Wnt signaling is to suppress PORCN function with synthetic inhibitors, which interrupt the secretion of Wnt ligands. Here, we tested the impact of two PORCN inhibitors on chondrogenesis. As a reference, we also used another Wnt signaling inhibitor - PF670462, which inhibits CK1$\delta$/1$\varepsilon$ downstream of the Wnt receptor complex,[36] and we uncovered distinct outcomes compared to PORCN manipulation.

### PORCN inhibition as stimulator of chondrogenic events

Our study demonstrates that PORCN inhibition has a substantial positive impact on early mesenchymal condensation

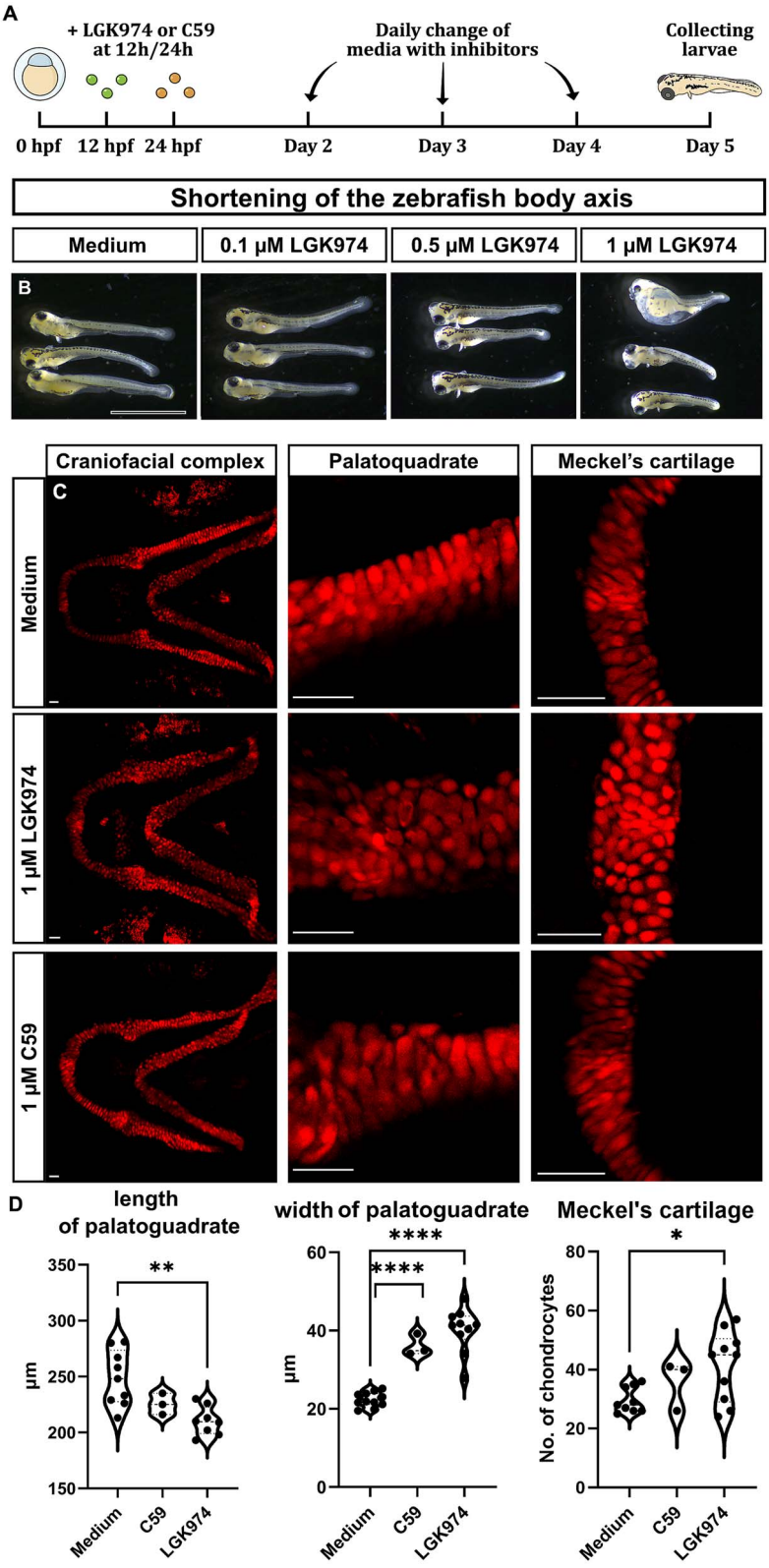


**Figure 8.** The effect of PORCN inhibitors on chondrogenesis in zebrafish embryos. (A) Schema of experimental design showing that PORCN inhibitors were added into zebrafish cultivation media at 0, 12, or 24 hpf to identify the effect of inhibitors during early embryogenesis or later during chondrogenesis in vivo. All embryos were collected at 5 dpf. (B) External morphology of zebrafish at stage 5 dpf. Increased concentration of LGK974 induced progressive shortening of the longitudinal axis of embryos in animals treated at 24 hpf. Scale bar = 2 mm. (C) Jaw cartilages of 4 dpf transgenic Sox10:DsRed zebrafish were shorter and thicker after cultivation with C59 or LGK974 (1 $\mu$M concentration added at 12 hpf) with a disrupted pattern of chondrocytes alignment. Scale bars: Lower view = 100 $\mu$m, details = 20 $\mu$m. (D) Analysis of palatoquadrate length, palatoquadrate width, and Meckel's cartilage following C59 and LGK974 treatment. Statistical analyses were performed using the Mann–Whitney test ($n = 6$). Abbrevation: PORCN, Porcupine.

in micromass cultures. Specifically, PORCN inhibition leads to an increased number of cartilaginous nodules and enhanced ECM production. This positive effect is attributed to the inhibition of Wnt/$\beta$-catenin signaling. These findings align with previous studies suggesting that Wnt signaling plays a pivotal role in directing mesenchymal progenitors toward either chondrocyte or osteoblast differentiation during early skeletogenesis.[1,5] For instance, inactivation of $\beta$-catenin in mouse micromasses has been shown to significantly promote chondrocyte differentiation.[5] Similarly, the application of DKK1, a well-known inhibitor of the canonical Wnt pathway, has been found to stimulate chondrogenesis in human mesenchymal stem cells.[71] Furthermore, other studies have demonstrated that Wnt inhibitors can stimulate cartilage regeneration in injured postnatal mouse cartilage, further supporting the therapeutic potential of modulating this pathway.[72]

Conversely, excessive activation of canonical Wnt signaling has been shown to hinder chondrocyte differentiation and even induce bone formation.[5,69,73] These studies suggest that maintaining a delicate balance in Wnt signaling is crucial for proper chondrogenesis and skeletal development. Our results reinforce the idea that PORCN inhibition, by disrupting canonical Wnt signaling, creates an environment conducive to chondrogenesis and cartilage formation. This highlights the therapeutic potential of targeting PORCN for cartilage regeneration, especially in contexts where canonical Wnt signaling is overly active and may be detrimental to cartilage development.

Members of non-canonical Wnt signaling, such as WNT5a, play a positive role in cartilage development by promoting the differentiation of cartilage progenitors during mesenchymal condensation.[6,11,53,67] This is consistent with our findings, where PORCN inhibition, which impacts both canonical and non-canonical Wnt signaling, enhances mesenchymal condensation and increases ECM production during the early stages of chondrogenesis. Our findings suggest that WNT5a signaling may be a key factor in modulating this effect, as PORCN inhibition can shift the balance between canonical and non-canonical Wnt pathways, making cells more responsive to WNT5a in specific contexts.

However, the positive effects of WNT5a in cartilage development appear to be temporary. Prolonged WNT5a treatment has been shown to stimulate ECM degradation and inhibit chondrocyte hypertrophy.[67,74] This temporary nature of WNT5a's beneficial effects highlights a key challenge in cartilage regeneration therapies: sustaining the initial pro-chondrogenic effects while avoiding detrimental impacts on cartilage maturation and hypertrophy. Our data suggest that the inhibition of PORCN may offer a solution to this issue by not only promoting the early stages of chondrogenesis (such as mesenchymal condensation and ECM production) but also by potentially regulating the timing of hypertrophic differentiation. By interfering with canonical Wnt signaling, PORCN inhibitors may mitigate the risk of excessive ECM degradation or premature hypertrophy associated with prolonged WNT5a exposure.

Moreover, the combination of PORCN inhibition with exogenous WNT5a treatment can offer a promising therapeutic approach to stimulate cartilage regeneration, especially in osteochondral defects. The ability of PORCN inhibitors to enhance early chondrogenesis, combined with controlled activation of non-canonical Wnt pathways, may help prolong the beneficial effects of WNT5a while attenuating its negative impact on ECM integrity and hypertrophy. Thus, this work not only advances our understanding of how Wnt signaling regulates chondrogenesis but also provides valuable insights into potential therapeutic strategies for cartilage repair and regeneration.

## Differential effects of PORCN inhibition on chondrocyte differentiation through Ihh regulation

In addition to the downregulation of the Wnt target gene *Axin2*,[51] one of the most striking molecular changes observed following PORCN inhibitor treatment was the dramatic upregulation of *Ihh*, a key marker of prehypertrophic chondrocytes.[55] *Ihh* plays a crucial role in regulating chondrocyte maturation and coordinating bone growth, particularly by promoting the transition from proliferative to hypertrophic chondrocytes.[75] PORCN influences Ihh signaling in chondrogenesis indirectly through its role in Wnt signaling modulation. The interaction between Wnt and Hedgehog (Hh) pathways is well-documented in skeletal development, with both signaling cascades tightly regulating chondrocyte proliferation, differentiation, and hypertrophy.[76]

The effect of PORCN inhibition on Ihh signaling can be explained by the relief of repression on Ihh due to the inhibition of canonical Wnt signaling. Canonical Wnt/$\beta$-catenin signaling plays a crucial role in cartilage development by inhibiting chondrocyte differentiation and suppressing *Ihh* expression.[70] When PORCN is inhibited, the secretion of all Wnt ligands is blocked, leading to a reduction in canonical Wnt signaling activity.[15,16] This, in turn, lifts the repression on *Ihh* expression, allowing chondrocytes to transition more rapidly from the proliferative to the prehypertrophic state. Consistently, our findings demonstrate a decrease in the proliferative zone alongside a significant increase in *Ihh* expression, further supporting this model. Moreover, previous in vivo studies demonstrated that *Ihh* overexpression accelerates early chondrocyte differentiation in developing long bones of mice,[77,78] aligning with our findings in tibiae organ cultures. By increasing Ihh expression, PORCN inhibitors push chondrocytes toward hypertrophy earlier, which is consistent with our observations of expanded prehypertrophic and hypertrophic zones in tibiae cultures.

Additionally, non-canonical WNT5a and WNT11 signaling have been shown to promote chondrogenesis by facilitating mesenchymal condensation and stimulating *Ihh* expression, which plays a crucial role in cartilage development.[79] On the other hand, Gli3A has been found to upregulate WNT5a expression during chondrocyte hypertrophy, suggesting a potential interplay between HH and WNT signaling pathways in regulating cartilage maturation.[80] While PORCN inhibition blocks the secretion of all Wnt ligands, potentially reducing non-canonical Wnt signaling initially, the suppression of canonical Wnt signaling may enhance cellular responsiveness to exogenous WNT5a. This effect was evident in our micromass experiments, where WNT5a treatment significantly promoted chondrogenesis in the presence of PORCN inhibitors. Since WNT5a is known to activate Ihh signaling,[79] this could explain why PORCN inhibition ultimately leads to increased *Ihh* expression in specific contexts.

Interestingly, the effects of PORCN inhibitors on *Ihh* expression appear to be stage- and context-dependent. While our data from micromass and tibiae cultures show a strong *Ihh* upregulation associated with enhanced chondrocyte

differentiation, studies utilizing IWP-2, another PORCN inhibitor, reported the opposite effect in human mesenchymal stem cells undergoing differentiation into articular chondrocytes.[81] Specifically, IWP-2 treatment led to a reduction in *Ihh* and *Col10* expression, ultimately resulting in a mild anti-hypertrophic and strong anti-osteogenic effect.[81] This discrepancy highlights that the impact of PORCN inhibition varies depending on the developmental stage and cellular context—suggesting that while PORCN inhibition accelerates chondrocyte maturation in the growth plate, it may have an inhibitory role in chondrocytes destined for articular cartilage formation.

These findings emphasize the complex and dynamic role of Wnt signaling in chondrogenesis, where PORCN inhibition modulates Ihh signaling indirectly by altering the balance between canonical and non-canonical Wnt pathways, triggering compensatory mechanisms, and accelerating the differentiation of chondrocytes. The stage- and context-specific nature of this interaction suggests that PORCN inhibitors may differentially regulate Ihh activity depending on developmental stage or cartilage type.

## Impact of PORCN inhibition on endochondral ossification

The application of PORCN inhibitors in our case resulted in stage-specific phenotypic changes that were also highly dependent on the tissue context. The observed effects varied based on the developmental timing of inhibitor administration, with earlier exposure leading to severe disruptions of cartilage formation (as observed in zebrafish) or cartilage expansion (as observed in tibia cultures) targeting different cellular processes.

Our findings demonstrate that PORCN inhibitors can significantly influence the later stages of endochondral ossification, as observed in mouse embryonic tibia cultures. Treatment with PORCN inhibitors led to a substantial increase in cartilaginous tissue and overall bone length, driven by the expansion of the hypertrophic zone. This bone elongation was facilitated by the expansion of the hypertrophic zone, while at the same time, the proliferative zone was markedly reduced. Although the initial effects of PORCN inhibition appear to promote bone lengthening, long-term consequences may include cartilage exhaustion. Proper postnatal bone elongation depends on the sustained proliferation of chondrocytes within the growth plate, ensuring a continuous supply of cells for endochondral ossification. If the balance between proliferation and differentiation is disrupted, the growth plate may become prematurely depleted, ultimately leading to bone growth defects.[1] This hypothesis is supported by clinical and genetic evidence. Focal dermal hypoplasia (FDH) patients, who carry mutations in PORCN, as well as mice with conditional PORCN inactivation in the limb mesenchyme, exhibit significant limb shortening, affecting both long bones and digits.[18,23] Similarly, mice with conditionally activated $\beta$-catenin demonstrated accelerated chondrocyte maturation in joints and the occurrence of a phenotype similar to osteoarthritis, further emphasizing the crucial role of Wnt signaling in skeletal development.

Proper bone growth requires precise, stage-specific regulation of Wnt signaling activity.[82] Depending on timing, dosage, and localization, Wnt pathway alterations can lead to either bone elongation or severe shortening, often associated with structural defects in the epiphyseal growth plate.[73,83–85] Indeed, mouse models with conditional *Porcn* inactivation in the limb mesenchyme display severely shortened long bones and digits, characterized by reduced ossification at the central zone and an expansion of distal cartilaginous components.[18,23] This suggests that Wnt-driven signaling gradients are essential for the spatial and temporal regulation of bone formation.

Taken together, our data reinforce the idea that PORCN inhibition affects multiple stages of chondrocyte differentiation, influencing the transition from cartilage to bone. These effects highlight the need for precise temporal control of Wnt signaling to ensure proper skeletal growth and development.

## Distinct role of PORCN in endochondral ossification of mammals and zebrafish

The development of craniofacial cartilages differs between mammals and zebrafish, and these differences are associated with differences in cartilage morphology and variations in Wnt signaling.[86,87] Mammalian craniofacial cartilage (eg, Meckel's cartilage, nasal cartilage) is primarily composed of type II collagen and aggrecan, similar to long bone cartilage, and is often a precursor to ossification.[88–90] Zebrafish craniofacial cartilage is characterized by a more flexible and less mineralized ECM compared to mammalian cartilage. This ECM composition includes not only type II collagen but also other components, such as collagen IX (Col9a1), collagen XI (Col11a1), and elastin, contributing to its unique structural properties.[91] In mammals, cranial neural crest (CNC)-derived mesenchymal cells differentiate into chondrocytes or osteoblasts, with Wnt/$\beta$-catenin signaling favoring osteogenesis, while in zebrafish, CNC-derived cells predominantly form persistent cartilage structures, which do not transition to bone as frequently as in mammals.[92] Blocking Wnt signaling in zebrafish, where cartilage is the primary fate, may disrupt proper craniofacial cartilage patterning rather than simply increasing chondrogenesis.

From a signaling point of view, canonical Wnt/$\beta$-catenin signaling in mammals acts as a key regulator of skeletal development by inhibiting chondrogenesis and promoting the differentiation of mesenchymal progenitors into osteoblasts rather than chondrocytes.[1,93] This pathway ensures a balance between cartilage formation and bone development, particularly in endochondral ossification. In contrast, zebrafish exhibit a different regulatory landscape, where Wnt signaling is less inhibitory toward chondrogenesis, allowing for more extensive cranial cartilage formation.[94] This difference is particularly evident in the development of craniofacial structures, where cartilage persists rather than being replaced by bone. Moreover, non-canonical Wnt signaling (wnt4a, wnt11r, wnt5b, wnt9a, and wnt11) plays a more prominent role in zebrafish craniofacial development, acting as a key driver of cartilage patterning and morphogenesis rather than directly regulating differentiation.[95–97] Similar to our results, altered global dimensions of Meckel's cartilage including significant shortening of cartilage was observed in wls, wnt5b, and gpc4 zebrafish mutant lines.[95,98] Moreover, Wnt mutants displayed disorganized primary cilia arrangements resulting in a malformed Meckel's cartilage arch. In these mutants, chondrocyte polarity appeared to be randomized, which was associated with differing cell shape and their organization similar to our animals.[98] This reliance on non-canonical Wnt

signaling in zebrafish probably contributed to observe misshaping of craniofacial cartilage.

In summary, PORCN inhibition disrupts both canonical and non-canonical Wnt signaling, leading to distinct effects in different models. In zebrafish, where non-canonical Wnt signaling dominates, inhibition causes craniofacial cartilage mispatterning and disorganization rather than simply enhancing chondrogenesis. This underscores the reliance of zebrafish craniofacial development on intact non-canonical signaling. In contrast, mammalian cartilage development, which is strongly regulated by canonical Wnt/$\beta$-catenin signaling, shifts toward chondrogenesis upon PORCN inhibition, reinforcing hypertrophic cartilage formation. These differences highlight the need for caution when extrapolating zebrafish findings to mammals. Additionally, our data demonstrate that PORCN inhibition elicits tissue-specific responses in vivo, likely due to variations in Wnt signaling activity across developmental stages and anatomical regions. While some tissues show increased chondrogenesis, others experience structural disruptions, emphasizing the complex, context-dependent role of PORCN in cartilage development and its implications for regenerative medicine and skeletal disorders.

## Conclusion

Our study explores the effect of PORCN inhibition on chondrogenesis. We demonstrate that PORCN plays a pivotal role in multiple stages of cartilage development, primarily by regulating Wnt signaling. Specifically, PORCN inhibition enhances ECM production and potentially promotes proliferation during the early phases of chondrogenesis, while also driving premature chondrocyte hypertrophy at later stages in mammals. This dual effect underscores the essential role of PORCN in orchestrating key differentiation events throughout cartilage formation.

As aberrant regulation of chondrocyte hypertrophy can contribute to several skeletal disorders, such as osteoarthritis, osteopetrosis, chondrodysplasias, and skeletal dysplasias, understanding the factors regulating chondrocyte hypertrophy can enhance the development of new therapies for these conditions. Altering PORCN activity by clinical grade inhibitors could be efficiently used for fine-tuning chondrocyte differentiation and be employed as beneficial in tissue engineering or for enhancing cartilage regeneration.

## Acknowledgments

The authors would like to thank Lucie Vrlíková for their technical support.

## Author contributions

Michael Killinger (Methodology, Formal analysis, Investigation, Writing—original draft, Visualization), Tereza Szotkowská (Methodology, Formal analysis, Investigation, Writing—original draft, Visualization), Denisa Lusková (Methodology, Investigation), Nikodém Zezula (Methodology, Formal analysis, Investigation, Visualization), Vítězslav Bryja (Conceptualization, Resources, Writing—review & editing, Supervision, Funding acquisition), and Marcela Buchtová (Conceptualization, Resources, Writing—original draft, Writing—review & editing, Supervision, Funding acquisition)

Michael Killinger and Tereza Szotkowská contributed equally to this work.

## Supplementary material

Supplementary material is available at *JBMR Plus* online.

## Funding

This study was supported by the Ministry of Health (NW24-10-00204, M.B. lab), the Czech Science Foundation (19-28347X, V.B. lab) and the Ministry of Education, Youth and Sports of the Czech Republic from the Operational Programme Research, Development and Education (CZ.02.1.01/0.0/0.0/15_003/0000460).

## Conflicts of interest

The authors declare no conflict of interest.

## Data availability

The authors confirm that the data supporting the findings of this study are available within the article and its supplementary materials.

## References

1. Usami Y, Gunawardena AT, Iwamoto M, Enomoto-Iwamoto M. Wnt Signaling in cartilage development and diseases: lessons from animal studies. *Lab Investig*. 2016;96(2):186-196. https://doi.org/10.1038/labinvest.2015.142
2. Deshmukh V, Hu H, Barroga C, et al. A small-molecule inhibitor of the Wnt pathway (SM04690) as a potential disease modifying agent for the treatment of osteoarthritis of the knee. *Osteoarthr Cartil*. 2018;26(1):18-27. https://doi.org/10.1016/j.joca.2017.08.015
3. Hwang SG, Yu SS, Lee SW, Chun JS. Wnt-3a regulates chondrocyte differentiation via c-Jun/AP-1 pathway. *FEBS Lett*. 2005;579(21):4837-4842. https://doi.org/10.1016/j.febslet.2005.07.067
4. Mbalaviele G, Sheikh S, Stains JP, et al. B-catenin and BMP-2 synergize to promote osteoblast differentiation and new bone formation. *J Cell Biochem*. 2005;94(2):403-418. https://doi.org/10.1002/jcb.20253
5. Day TF, Guo X, Garrett-Beal L, Yang Y. Wnt/$\beta$-catenin Signaling in mesenchymal progenitors controls osteoblast and chondrocyte differentiation during vertebrate Skeletogenesis. *Dev Cell*. 2005;8(5):739-750. https://doi.org/10.1016/j.devcel.2005.03.016
6. Yang Y, Topol L, Lee H, Wu J. Wnt5a and Wnt5b exhibit distinct activities in coordinating chondrocyte proliferation and differentiation. *Development*. 2003;130(5):1003-1015. https://doi.org/10.1242/dev.00324
7. Gao B, Song H, Bishop K, et al. Wnt signaling gradients establish planar cell polarity by inducing Vangl2 phosphorylation through Ror2. *Dev Cell*. 2011;20(2):163-176. https://doi.org/10.1016/j.devcel.2011.01.001
8. Gao B, Ajima R, Yang W, et al. Coordinated directional outgrowth and pattern formation by integration of Wnt5a and Fgf signaling in planar cell polarity. *Development*. 2018;145(8):1-14. https://doi.org/10.1242/dev.163824
9. Duprez D, Leyns L, Bonnin MA, et al. Expression of Frzb-1 during chick development. *Mech Dev*. 1999;89(1-2):179-183. https://doi.org/10.1016/S0925-4773(99)00206-3
10. Enomoto-Iwamoto M, Kitagaki J, Koyama E, et al. The Wnt antagonist Frzb-1 regulates chondrocyte maturation and long bone development during limb skeletogenesis. *Dev Biol*. 2002;251(1):142-156. https://doi.org/10.1006/dbio.2002.0802
11. Hartmann C, Tabin CJ. Dual roles of Wnt signaling during chondrogenesis in the chicken limb. *Development*. 2000;127(14):3141-3159. https://doi.org/10.1242/dev.127.14.3141
12. Hartmann C, Tabin CJ. Wnt-14 plays a pivotal role in inducing synovial joint formation in the developing appendicular skeleton.

*Cell*. 2001;104(3):341-351. https://doi.org/10.1016/S0092-8674(01)00222-7
13. Rudnicki JA, Brown AMC. Inhibition of chondrogenesis by Wnt gene expression in vivo and in vitro. *Dev Biol*. 1997;185(1):104-118. https://doi.org/10.1006/dbio.1997.8536
14. Hofmann K. A superfamily of membrane-bound O-acyltransferases with implications for Wnt signaling. *Trends Biochem Sci*. 2000;25(3):111-112. https://doi.org/10.1016/S0968-0004(99)01539-X
15. Tanaka K, Okabayashi K, Asashima M, Perrimon N, Kadowaki T. The evolutionarily conserved porcupine gene family is involved in the processing of the Wnt family. *Eur J Biochem*. 2000;267(13):4300-4311. https://doi.org/10.1046/j.1432-1033.2000.01478.x
16. Takada R, Satomi Y, Kurata T, et al. Monounsaturated fatty acid modification of Wnt protein: its role in Wnt secretion. *Dev Cell*. 2006;11(6):791-801. https://doi.org/10.1016/j.devcel.2006.10.003
17. Herr P, Basler K. Porcupine-mediated lipidation is required for Wnt recognition by Wls. *Dev Biol*. 2012;361(2):392-402. https://doi.org/10.1016/j.ydbio.2011.11.003
18. Barrott JJ, Cash GM, Smith AP, Barrow JR, Murtaugh LC. Deletion of mouse Porcn blocks Wnt ligand secretion and reveals an ectodermal etiology of human focal dermal hypoplasia/Goltz syndrome. *Proc Natl Acad Sci USA*. 2011;108(31):12752-12757. https://doi.org/10.1073/pnas.1006437108
19. Biechele S, Cox BJ, Rossant J. Porcupine homolog is required for canonical Wnt signaling and gastrulation in mouse embryos. *Dev Biol*. 2011;355(2):275-285. https://doi.org/10.1016/j.ydbio.2011.04.029
20. Chen Q, Takada R, Takada S. Loss of porcupine impairs convergent extension during gastrulation in zebrafish. *J Cell Sci*. 2012;125(Pt 9):2224-2234. https://doi.org/10.1242/jcs.098368
21. Wang X, Reid Sutton V, Omar Peraza-Llanes J, et al. Mutations in X-linked PORCN, a putative regulator of Wnt signaling, cause focal dermal hypoplasia. *Nat Genet*. 2007;39(7):836-838. https://doi.org/10.1038/ng2057
22. Yu M, Qin K, Fan J, et al. The evolving roles of Wnt signaling in stem cell proliferation and differentiation, the development of human diseases, and therapeutic opportunities. *Genes Dis*. 2023;11(3):101026. https://doi.org/10.1016/j.gendis.2023.04.042
23. Liu W, Shaver TM, Balasa A, et al. Deletion of Porcn in mice leads to multiple developmental defects and models human focal dermal hypoplasia (Goltz syndrome). *PLoS One*. 2012;7(3):e32331. https://doi.org/10.1371/journal.pone.0032331
24. Arlt A, Kohlschmidt N, Hentschel A, et al. Novel insights into PORCN mutations, associated phenotypes and pathophysiological aspects. *Orphanet J Rare Dis*. 2022;17(1):29. https://doi.org/10.1186/s13023-021-02068-w
25. Funck-Brentano T, Nilsson KH, Brommage R, et al. Porcupine inhibitors impair trabecular and cortical bone mass and strength in mice. *J Endocrinol*. 2018;238(1):13-23. https://doi.org/10.1530/JOE-18-0153
26. Lawson LY, Brodt MD, Migotsky N, Chermside-Scabbo CJ, Palaniappan R, Silva MJ. Osteoblast-specific Wnt secretion is required for skeletal homeostasis and loading-induced bone formation in adult mice. *J Bone Miner Res*. 2022;37(1):108-120. https://doi.org/10.1002/jbmr.4445
27. Feng J, Zhang Q, Pu F, et al. Signalling interaction between β-catenin and other signalling molecules during osteoarthritis development. *Cell Prolif*. 2024;57(6):e13600. https://doi.org/10.1111/cpr.13600
28. von Maltzahn J, Chang NC, Bentzinger CF, Rudnicki MA. Wnt signaling in myogenesis. *Trends Cell Biol*. 2012;22(11):602-609. https://doi.org/10.1016/j.tcb.2012.07.008
29. Hall EH, Terezhalmy GT. Focal dermal hypoplasia syndrome: case report and literature review. *J Am Acad Dermatol*. 1983;9(3):443-451. https://doi.org/10.1016/S0190-9622(83)70157-X
30. Maas SM, Lombardi MP, van Essen AJ, et al. Phenotype and genotype in 17 patients with Goltz–Gorlin syndrome. *J Med Genet*. 2009;46(10):716-720. https://doi.org/10.1136/jmg.2009.068403
31. Temple IK, MacDowall P, Baraitser M, Atherton DJ. Focal dermal hypoplasia (Goltz syndrome). *J Med Genet*. 1990;27(3):180-187. https://doi.org/10.1136/jmg.27.3.180
32. Proffitt KD, Virshup DM. Precise regulation of porcupine activity is required for physiological Wnt signaling. *J Biol Chem*. 2012;287(41):34167-34178. https://doi.org/10.1074/jbc.M112.381970
33. Shah K, Panchal S, Patel B. Porcupine inhibitors: novel and emerging anti-cancer therapeutics targeting the Wnt signaling pathway. *Pharmacol Res*. 2021;167:105532. https://doi.org/10.1016/j.phrs.2021.105532
34. Cheng D, Zhang G, Han D, Gao W, Pan S. N-(hetero)aryl, 2-(hetero)aryl-substituted acetamides for use as Wnt signaling modulators. Published online September 10, 2010. Accessed February 15, 2025. https://patents.google.com/patent/WO2010101849A1/en
35. Liu J, Pan S, Hsieh MH, et al. Targeting Wnt-driven cancer through the inhibition of porcupine by LGK974. *Proc Natl Acad Sci USA*. 2013;110(50):20224-20229. https://doi.org/10.1073/pnas.1314239110
36. Janovská P, Normant E, Miskin H, Bryja V. Targeting casein kinase 1 (CK1) in hematological cancers. *Int J Mol Sci*. 2020;21(23):9026. https://doi.org/10.3390/ijms21239026
37. Janovska P, Verner J, Kohoutek J, et al. Casein kinase 1 is a therapeutic target in chronic lymphocytic leukemia. *Blood*. 2018;131(11):1206-1218. https://doi.org/10.1182/blood-2017-05-786947
38. Walton KM, Fisher K, Rubitski D, et al. Selective inhibition of casein kinase 1 epsilon minimally alters circadian clock period. *J Pharmacol Exp Ther*. 2009;330(2):430-439. https://doi.org/10.1124/jpet.109.151415
39. Meng QJ, Maywood ES, Bechtold DA, et al. Entrainment of disrupted circadian behavior through inhibition of casein kinase 1 (CK1) enzymes. *Proc Natl Acad Sci USA*. 2010;107(34):15240-15245. https://doi.org/10.1073/pnas.1005101107
40. Li X, Han Y, Li G, Zhang Y, Wang J, Feng C. Role of Wnt signaling pathway in joint development and cartilage degeneration. *Front Cell Dev Biol*. 2023;11:1181619. https://doi.org/10.3389/fcell.2023.1181619
41. Hamburger V, Hamilton HL. A series of normal stages in the development of the chick embryo. *Dev Dyn*. 1992;195(4):231-272. https://doi.org/10.1002/aja.1001950404
42. Killinger M, Kratochvilová A, Reihs EI, Matalová E, Klepárník K, Rothbauer M. Microfluidic device for enhancement and analysis of osteoblast differentiation in three-dimensional cell cultures. *J Biol Eng*. 2023;17(1):77. https://doi.org/10.1186/s13036-023-00395-z
43. Kozhemyakina E, Lassar AB, Zelzer E. A pathway to bone: signaling molecules and transcription factors involved in chondrocyte development and maturation. *Development*. 2015;142(5):817-831. https://doi.org/10.1242/dev.105536
44. Lauing KL, Cortes M, Domowicz MS, Henry JG, Baria AT, Schwartz NB. Aggrecan is required for growth plate cytoarchitecture and differentiation. *Dev Biol*. 2014;396(2):224-236. https://doi.org/10.1016/j.ydbio.2014.10.005
45. Mello MA, Tuan RS. High density micromass cultures of embryonic limb bud mesenchymal cells: an in vitro model of endochondral skeletal development. *In Vitro Cell Dev Biol Anim*. 1999;35(5):262-269. https://doi.org/10.1007/s11626-999-0070-0
46. Daniels K, Reiter R, Solursh M. Chapter 12 micromass cultures of limb and other mesenchyme. In: Bronner-Fraser M, ed. *Methods in Cell Biology. Vol 51. Methods in Avian Embryology*. Academic Press; 1996:237-247 10.1016/S0091-679X(08)60631-7.
47. Akiyama H, Lyons JP, Mori-Akiyama Y, et al. Interactions between Sox9 and β-catenin control chondrocyte differentiation. *Genes Dev*. 2004;18(9):1072-1087. https://doi.org/10.1101/gad.1171104

48. Ng LJ, Wheatley S, Muscat GEO, et al. SOX9 binds DNA, activates transcription, and coexpresses with type II collagen during chondrogenesis in the mouse. *Dev Biol*. 1997;183(1):108-121. https://doi.org/10.1006/dbio.1996.8487
49. Tacchetti C, Tavella S, Dozin B, Quarto R, Robino G, Cancedda R. Cell condensation in chondrogenic differentiation. *Exp Cell Res*. 1992;200(1):26-33. https://doi.org/10.1016/S0014-4827(05)80067-9
50. Aulthouse AL, Solursh M. The detection of a precartilage, blastema-specific marker. *Dev Biol*. 1987;120(2):377-384. https://doi.org/10.1016/0012-1606(87)90240-5
51. Jho E-H, Zhang T, Domon C, Joo CK, Freund JN, Costantini F. Wnt/$\beta$-catenin/Tcf signaling induces the transcription of Axin2, a negative regulator of the signaling pathway. *Mol Cell Biol*. 2002;22(4):1172-1183. https://doi.org/10.1128/MCB.22.4.1172-1183.2002
52. Torres VI, Godoy JA, Inestrosa NC. Modulating Wnt signaling at the root: porcupine and Wnt acylation. *Pharmacol Ther*. 2019;198(June):34-45. https://doi.org/10.1016/j.pharmthera.2019.02.009
53. Ma B, Landman EBM, Miclea RL, et al. WNT Signaling and cartilage: of mice and men. *Calcif Tissue Int*. 2013;92(5):399-411. https://doi.org/10.1007/s00223-012-9675-5
54. Akiyama H, Chaboissier MC, Martin JF, Schedl A, de Crombrugghe B. The transcription factor Sox9 has essential roles in successive steps of the chondrocyte differentiation pathway and is required for expression of Sox5 and Sox6. *Genes Dev*. 2002;16(21):2813-2828. https://doi.org/10.1101/gad.1017802
55. St-Jacques B, Hammerschmidt M, McMahon AP. Indian hedgehog signaling regulates proliferation and differentiation of chondrocytes and is essential for bone formation. *Genes Dev*. 1999;13(16):2072-2086.
56. Humke EW, Dorn KV, Milenkovic L, Scott MP, Rohatgi R. The output of hedgehog signaling is controlled by the dynamic association between suppressor of fused and the Gli proteins. *Genes Dev*. 2010;24(7):670-682. https://doi.org/10.1101/gad.1902910
57. Engsig MT, Chen QJ, Vu TH, et al. Matrix metalloproteinase 9 and vascular endothelial growth factor are essential for osteoclast recruitment into developing long bones. *J Cell Biol*. 2000;151(4):879-889.
58. Zoch ML, Clemens TL, Riddle RC. New insights into the biology of osteocalcin. *Bone*. 2016;82(Jan):42-49. https://doi.org/10.1016/j.bone.2015.05.046
59. Sánchez-Porras D, Durand-Herrera D, Paes AB, et al. Ex vivo generation and characterization of human hyaline and elastic cartilaginous microtissues for tissue engineering applications. *Biomedicines*. 2021;9(3):292. https://doi.org/10.3390/biomedicines9030292
60. Irie Y, Mizumoto H, Fujino S, Kajiwara T. Development of articular cartilage grafts using organoid formation techniques. *Transplant Proc*. 2008;40(2):631-633. https://doi.org/10.1016/j.transproceed.2008.01.024
61. Sun Y, Wu Q, Dai K, You Y, Jiang W. Generating 3D-cultured organoids for pre-clinical modeling and treatment of degenerative joint disease. *Sig Transduct Target Ther*. 2021;6(1):380-384. https://doi.org/10.1038/s41392-021-00675-4
62. Matchkov VV, Krivoi II. Specialized functional diversity and interactions of the Na, K-ATPase. *Front Physiol*. 2016;7:179.
63. Aghajanian P, Mohan S. The art of building bone: emerging role of chondrocyte-to-osteoblast transdifferentiation in endochondral ossification. *Bone Res*. 2018;6(1):1-9. https://doi.org/10.1038/s41413-018-0021-z
64. Yang K, Hitomi M, Stacey DW. Variations in cyclin D1 levels through the cell cycle determine the proliferative fate of a cell. *Cell Div*. 2006;1(1):32. https://doi.org/10.1186/1747-1028-1-32
65. Goldring MB, Tsuchimochi K, Ijiri K. The control of chondrogenesis. *J Cell Biochem*. 2006;97(1):33-44. https://doi.org/10.1002/jcb.20652
66. Long F, Ornitz DM. Development of the endochondral skeleton. *Cold Spring Harb Perspect Biol*. 2013;5(1):a008334. https://doi.org/10.1101/cshperspect.a008334
67. Church V, Nohno T, Linker C, Marcelle C, Francis-West P. Wnt regulation of chondrocyte differentiation. *J Cell Sci*. 2002;115(24):4809-4818. https://doi.org/10.1242/jcs.00152
68. Hartmann C. Wnt-signaling and skeletogenesis. *J Musculoskelet Neuronal Interact*. 2002;2(3):274-276
69. Nalesso G, Sherwood J, Bertrand J, et al. WNT-3A modulates articular chondrocyte phenotype by activating both canonical and noncanonical pathways. *J Cell Biol*. 2011;193(3):551-564. https://doi.org/10.1083/jcb.201011051
70. Später D, Hill TP, O'Sullivan RJ, Gruber M, Conner DA, Hartmann C. Wnt9a signaling is required for joint integrity and regulation of Ihh during chondrogenesis. *Development*. 2006;133(15):3039-3049. https://doi.org/10.1242/dev.02471
71. Im GI, Quan Z. The effects of Wnt inhibitors on the chondrogenesis of human mesenchymal stem cells. *Tissue Eng A*. 2010;16(7):2405-2413. https://doi.org/10.1089/ten.tea.2009.0359
72. Bastakoty D, Saraswati S, Cates J, Lee E, Nanney LB, Young PP. Inhibition of Wnt/$\beta$-catenin pathway promotes regenerative repair of cutaneous and cartilage injury. *FASEB J*. 2015;29(12):4881-4892. https://doi.org/10.1096/fj.15-275941
73. Yuasa T, Otani T, Koike T, Iwamoto M, Enomoto-Iwamoto M. Wnt/$\beta$-catenin signaling stimulates matrix catabolic genes and activity in articular chondrocytes: its possible role in joint degeneration. *Lab Investig*. 2008;88(3):264-274. https://doi.org/10.1038/labinvest.3700747
74. Daumer KM, Tufan AC, Tuan RS. Long-term in vitro analysis of limb cartilage development: involvement of Wnt signaling. *J Cell Biochem*. 2004;93(3):526-541. https://doi.org/10.1002/jcb.20190
75. Long F, Chung U, Ohba S, McMahon J, Kronenberg HM, McMahon AP. Ihh signaling is directly required for the osteoblast lineage in the endochondral skeleton. *Development*. 2004;131(6):1309-1318. https://doi.org/10.1242/dev.01006
76. Mak KK, Chen MH, Day TF, Chuang PT, Yang Y. Wnt/beta-catenin signaling interacts differentially with Ihh signaling in controlling endochondral bone and synovial joint formation. *Development*. 2006;133(18):3695-3707. https://doi.org/10.1242/dev.02546
77. Kobayashi T, Soegiarto DW, Yang Y, et al. Indian hedgehog stimulates periarticular chondrocyte differentiation to regulate growth plate length independently of PTHrP. *J Clin Invest*. 2005;115(7):1734-1742. https://doi.org/10.1172/JCI24397
78. Mak KK, Kronenberg HM, Chuang PT, Mackem S, Yang Y. Indian hedgehog signals independently of PTHrP to promote chondrocyte hypertrophy. *Development*. 2008;135(11):1947-1956. https://doi.org/10.1242/dev.018044
79. Diederichs S, Tonnier V, März M, Dreher SI, Geisbüsch A, Richter W. Regulation of WNT5A and WNT11 during MSC in vitro chondrogenesis: WNT inhibition lowers BMP and hedgehog activity, and reduces hypertrophy. *Cell Mol Life Sci*. 2019;76(19):3875-3889. https://doi.org/10.1007/s00018-019-03099-0
80. Wuelling M, Schneider S, Schröther VA, Waterkamp C, Hoffmann D, Vortkamp A. Wnt5a is a transcriptional target of Gli3 and Trps1 at the onset of chondrocyte hypertrophy. *Dev Biol*. 2020;457(1):104-118. https://doi.org/10.1016/j.ydbio.2019.09.012
81. Dreher SI, Fischer J, Walker T, Diederichs S, Richter W. Significance of MEF2C and RUNX3 regulation for endochondral differentiation of human mesenchymal progenitor cells. *Front Cell Dev Biol*. 2020;8:81. https://doi.org/10.3389/fcell.2020.00081
82. Regard JB, Zhong Z, Williams BO, Yang Y. Wnt Signaling in bone development and disease: making stronger bone with Wnts. *Cold Spring Harb Perspect Biol*. 2012;4(12):a007997. https://doi.org/10.1101/cshperspect.a007997
83. Yuasa T, Kondo N, Yasuhara R, et al. Transient activation of Wnt/$\beta$-catenin Signaling induces abnormal growth plate closure and articular cartilage thickening in postnatal mice. *Am*

*J Pathol*. 2009;175(5):1993-2003. https://doi.org/10.2353/ajpath.2009.081173
84. Houben A, Kostanova-Poliakova D, Weissenböck M, et al. B-catenin activity in late hypertrophic chondrocytes locally orchestrates osteoblastogenesis and osteoclastogenesis. *Development*. 2016;143(20):3826-3838. https://doi.org/10.1242/dev.137489
85. Golovchenko S, Hattori T, Hartmann C, et al. Deletion of beta catenin in hypertrophic growth plate chondrocytes impairs trabecular bone formation. *Bone*. 2013;55(1):102-112. https://doi.org/10.1016/j.bone.2013.03.019
86. Mallatt J. The origin of the vertebrate jaw: neoclassical ideas versus newer, development-based ideas. *Zoolog Sci*. 2008;25(10):990-998. https://doi.org/10.2108/zsj.25.990
87. Mork L, Crump G. Zebrafish craniofacial development: a window into early patterning. *Curr Top Dev Biol*. 2015;115:235-269. https://doi.org/10.1016/bs.ctdb.2015.07.001
88. Ababneh KT, Al-Khateeb TH. Immunolocalization of proteoglycans in Meckel's cartilage of the rat. *Open Dent J*. 2009;3(1):177-183. https://doi.org/10.2174/1874210600903010177
89. Shimo T, Kanyama M, Wu C, et al. Expression and roles of connective tissue growth factor in Meckel's cartilage development. *Dev Dyn*. 2004;231(1):136-147. https://doi.org/10.1002/dvdy.20109
90. Silbermann M, von der Mark K. An immunohistochemical study of the distribution of matrical proteins in the mandibular condyle of neonatal mice. I. Collagens. *J Anat*. 1990;170:11-22.
91. Baas D, Malbouyres M, Haftek-Terreau Z, Le Guellec D, Ruggiero F. Craniofacial cartilage morphogenesis requires zebrafish col11a1 activity. *Matrix Biol*. 2009;28(8):490-502. https://doi.org/10.1016/j.matbio.2009.07.004
92. Piotrowski T, Schilling TF, Brand M, et al. Jaw and branchial arch mutants in zebrafish II: anterior arches and cartilage differentiation. *Development*. 1996;123(1):345-356. https://doi.org/10.1242/dev.123.1.345
93. Hu L, Chen W, Qian A, Li YP. Wnt/$\beta$-catenin signaling components and mechanisms in bone formation, homeostasis, and disease. *Bone Res*. 2024;12(1):1-33. https://doi.org/10.1038/s41413-024-00342-8
94. Brunt LH, Begg K, Kague E, Cross S, Hammond CL. Wnt signalling controls the response to mechanical loading during zebrafish joint development. *Development*. 2017;144(15):2798-2809. https://doi.org/10.1242/dev.153528
95. Sisson BE, Dale RM, Mui SR, Topczewska JM, Topczewski J. A role of glypican4 and wnt5b in chondrocyte stacking underlying craniofacial cartilage morphogenesis. *Mech Dev*. 2015;138(Pt 3):279-290. https://doi.org/10.1016/j.mod.2015.10.001
96. Curtin E, Hickey G, Kamel G, Davidson AJ, Liao EC. Zebrafish wnt9a is expressed in pharyngeal ectoderm and is required for palate and lower jaw development. *Mech Dev*. 2011;128(1-2):104-115. https://doi.org/10.1016/j.mod.2010.11.003
97. Choe CP, Collazo A, Trinh LA, Pan L, Moens CB, Crump JG. Wnt-dependent epithelial transitions drive pharyngeal pouch formation. *Dev Cell*. 2013;24(3):296-309. https://doi.org/10.1016/j.devcel.2012.12.003
98. Ling IT, Rochard L, Liao EC. Distinct requirements of wls, wnt9a, wnt5b and gpc4 in regulating chondrocyte maturation and timing of endochondral ossification. *Dev Biol*. 2017;421(2):219-232. https://doi.org/10.1016/j.ydbio.2016.11.016


*JBMR Plus*, 2025, 9_ziaf048
https://doi.org/10.1093/jbmrpl/ziaf048
Research Article